NACA TN 4386

NATIONAL ADVISORY COMMITTEE FOR AERONAUTICS

TECHNICAL NOTE 4386

AN ANALYSIS OF RAMJET ENGINES USING SUPERSONIC COMBUSTION

By Richard J. Weber and John S. MacKay

Lewis Flight Propulsion Laboratory
Cleveland, Ohio

Washington

September 1958

NATIONAL ADVISORY COMMITTEE FOR AERONAUTICS

TECHNICAL NOTE 4386

AN ANALYSIS OF RAMJET ENGINES USING SUPERSONIC COMBUSTION

By Richard J. Weber and John S. MacKay

SUMMARY

Based on the assumption that shock-free internal burning is possible in a supersonic airstream, calculations are made for the performance of ramjets using supersonic combustion velocities.

Diffusion of the air from the flight speed to a lower supersonic velocity is generally found to be desirable before the air enters the combustor. With a constant-area combustor, both maximum thrust and over-all engine efficiency are achieved when sufficient heat is added to choke the flow at the combustor exit.

In the flight Mach number range considered, from 4 to 7, the over-all efficiency of both the supersonic-combustion and the conventional ramjet engines increases with flight speed. When compared with a conventional engine having a two-cone inlet, the supersonic-combustion engine with a Pitot inlet is less efficient at all speeds, with a wedge inlet is more efficient above Mach 7, and with an isentropic inlet is more efficient above Mach 5. At Mach 7, the maximum over-all efficiency is 45 and 54 percent for the wedge and isentropic inlets, respectively.

When simplified weight estimates are used, no weight advantage is found for the supersonic-combustion engine, as compared with the conventional ramjet.

INTRODUCTION

In a conventional ramjet, air is captured and decelerated to a low subsonic velocity by an inlet diffuser, after which heat is added in a combustor. Inasmuch as adding heat to a supersonic stream decelerates the flow and raises the static pressure, the possibility of replacing the conventional ramjet inlet and combustor by a combustor having a supersonic inlet velocity is thus suggested; this would compress the air thermodynamically, coincidently with the heat release.

Burning in a supersonic stream must always cause a relatively large total-pressure drop; whereas, at least ideally, the diffusion and subsequent subsonic combustion in a conventional ramjet may be accomplished with a vanishingly small total-pressure loss. In some cases, however, the supersonic-combustion ramjet may prove to be more efficient than a conventional ramjet that has finite diffusion losses. Another factor is that the lower static temperatures associated with supersonic combustion inhibit dissociation and thus reduce possible losses due to nonequilibrium nozzle expansion. In addition, supersonic combustion may tend to ease the cooling problems of the conventional engine.

The practical problems of employing supersonic combustion are very great: It is necessary to capture a stream tube of supersonic air, inject fuel, achieve a fairly uniform mixture of fuel and air, and carry out the combustion process - all in a reasonable length and preferably without causing a normal shock within the engine. There is currently no conclusive evidence that these requirements can be met; nevertheless, the present study starts with the basic assumption that stable supersonic combustion in an engine is possible. Granting such an assumption, the purpose of this report is to analyze the performance of supersonic-combustion ramjet cycles, to determine the effect of various design parameters, and to compare this performance with that of conventional ramjets. The thrust and efficiency of design-point engines operating at flight Mach numbers of 4 through 7 are calculated. Parameters studied include inlet type, combustion temperature, combustor area ratio, combustor cooling load, mass addition, wall friction, nozzle expansion ratio and velocity coefficient, and frozen against equilibrium nozzle expansion. Estimates of engine weights are made.

The preliminary calculations were made for an ideal gas with constant specific heat. An IBM 650 computer was used to make further calculations that took into account variations in specific heats. Hydrogen fuel was assumed. The results are presented in terms of over-all engine efficiency and thus are independent of the heating value of the actual fuel used.

The concept of supersonic combustion is by no means new, although little work appears to have been published on the subject. For example, an analysis of supersonic combustion to provide lift under a wing is given in reference 1. Reference 2 discusses applications to hypersonic ramjets being studied at the University of Michigan.

SYMBOLS

The following symbols are used in this report:

A	cross-sectional area, sq ft
$(A_6)_{full}$	fully expanded nozzle-exit area

C_F	thrust coefficient, F/q_0A
C_V	nozzle velocity coefficient
CRJ	conventional ramjet with subsonic combustion
c_p	specific heat at constant pressure, Btu/(lb)(^oR)
D	diameter, ft
F	net thrust (jet thrust minus inlet momentum), lb
f/a	fuel-air ratio
f	wall friction drag coefficient
H	lower heating value, Btu/lb
J	mechanical equivalent of heat, 778.2 ft-lb/Btu
L	length, ft
M	Mach number
m/a	weight ratio of injected fluid to air
n	wall pressure parameter
P	total pressure, lb/sq ft
p	static pressure, lb/sq ft
Q	heat flow, Btu/sec
q	incompressible dynamic head, $\frac{1}{2}\rho V^2$, lb/sq ft
S	entropy, Btu/(lb)(^oR)
SCRJ	supersonic combustion ramjet
sfc	specific fuel consumption, lb/(lb)(hr)
T	total temperature
t	static temperature
V	velocity, ft/sec

W	engine weight, lb
w_a	airflow rate, lb/sec
γ	ratio of specific heats
λ	wedge angle, deg
η_c	combustion efficiency, (ratio of actual-to-ideal fuel-air ratios)
η_e	over-all engine efficiency, $FV_0/(f/a)\ w_a H$
η_T	thermal efficiency
Ω	cycle work, Btu/lb

Subscripts:

c	combustor
d	diffuser
max	maximum
N	nozzle
s	skin
0	diffuser inlet
2	combustor inlet
4	combustor exit
5	nozzle throat
6	nozzle exit

ANALYSIS

Theory

Almost all steady-flow jet engines follow more or less approximately a Brayton cycle, that is, isentropic compression, constant-pressure combustion, and isentropic expansion. In contrast, the supersonic-combustion ramjet (SCRJ) may have no preliminary compression at all, and the

combustion pressure varies over a wide range. Because of these unusual features, some discussion of the basic thermodynamic cycle appears desirable.

General cycle. - The SCRJ cycle may be conveniently illustrated by a temperature-entropy diagram, as in figure 1. Air is initially at ambient temperature and pressure (point 0) and is flowing at a supersonic velocity (relative to the engine) equal to the flight speed. In the general case, the air is decelerated by a diffuser to some lower but still supersonic Mach number, path 0-1. The indicated increase in entropy can be shown to be related directly to a loss in total pressure. A path of constant momentum is then constructed through point 1; this line (generally called a Rayleigh line) represents a heat-addition process in a frictionless, constant-area duct. The lower branch of the Rayleigh line corresponds to supersonic Mach numbers and the upper branch to subsonic Mach numbers. As heat is added to the air, path 1-P is traced, resulting in a rise in static pressure and temperature and a reduction in Mach number. The area under the path is directly proportional to the amount of heat added (which is a function of the fuel-air ratio). The combustion process may be terminated at any point P. Provided the stoichiometric fuel-air ratio is not reached first, the heat addition may be continued up to the maximum entropy condition on the Rayleigh line (point 4). At this point the flow is choked; that is, the Mach number is 1, and no further heat can be added without changing the combustor-inlet conditions. The total amount of heat added by combustion is proportional to areas C + D in this case. Expansion of the hot gas takes place through a nozzle with a further increase in entropy due to friction (path 4-6). To close the cycle, heat is imagined to be rejected at constant pressure along path 6-0; the quantity of rejected heat is proportional to areas E + B + D.

The net cycle work Ω is equal to the difference between the heat added and the heat rejected. Cycle work here means the increase in kinetic energy produced in the air flowing through the engine. Since the engine thrust is proportional to the change in air velocity, the cycle work is a measure of the thrust produced. The work output of the cycle is less than the energy added in the form of heat; the ratio of the two quantities is defined as the thermal efficiency η_T. Not all the cycle work can be usefully applied to propelling the airplane, since some of the jet kinetic energy remains in the atmosphere in the form of turbulence after the airplane has flown by. The proportion of useful airplane work to cycle work is defined as the propulsive efficiency, which cannot be represented on the temperature-entropy diagram. The product of the thermal and propulsive efficiencies is defined as the over-all engine efficiency and is thus equal to the proportion of the fuel chemical energy that is effectively employed in propelling the airplane.

Based on the preceding definitions, the cycle work and the thermal efficiency may be expressed in terms of the areas on the temperature-entropy diagram as

$$\mathfrak{Q} = C - (E + B) \tag{1}$$

$$\eta_T = \frac{\mathfrak{Q}}{C + D} = 1 - \frac{1}{1 + \frac{C}{D}} - \frac{E + B}{C + D} \tag{2}$$

Reducing $E + B$ (by more efficient compression and expansion processes) improves both $\mathfrak{Q}$ and η_T (eq. (1)). Also, as seen from equation (2), increasing the ratio C/D improves η_T (provided the relative inlet and exit losses do not change). One possibility for increasing the C/D ratio is to provide more initial diffusion.

Supersonic diffusion. - In figure 1, some form of supersonic diffusion was assumed to take place before burning. The effect of such diffusion is indicated in figure 2 (for clarity, the inlet and exit losses are not shown). A cycle with no diffusion is given by path 0-4-6-0. A cycle employing diffusion follows path 0-1-4'-6'-0. In both cases, the net cycle work is represented by the crosshatched areas.

Figure 2 does not show whether small amounts of diffusion will increase or reduce the cycle work. In the limit, however, the air is diffused to Mach 1, at which point no heat may be added in a constant-area duct, and so the thrust becomes zero. It may be concluded, therefore, that sufficiently large amounts of diffusion necessarily will reduce the cycle work.

With regard to the efficiency, the following argument is presented to indicate that small amounts of diffusion are beneficial. Consider two narrow strips of area in the vicinity of point 4 and 4'. The C/D ratio for each of these strips is approximately given by

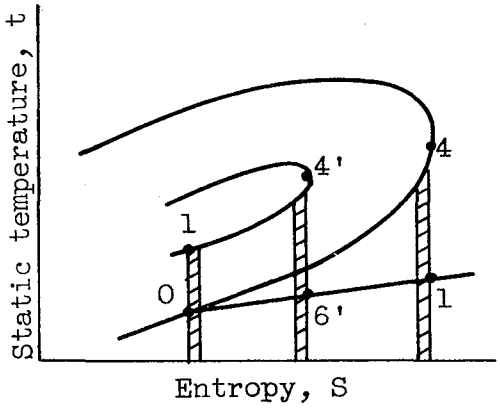

$$\left(\frac{C}{D}\right)_4 = \frac{t_4 - t_6}{t_6} = \left(\frac{p_4}{p_6}\right)^{\frac{\gamma-1}{\gamma}} - 1 \tag{3a}$$

$$\left(\frac{C}{D}\right)_{4'} = \frac{t_4' - t_6'}{t_6'} = \left(\frac{p_4'}{p_6'}\right)^{\frac{\gamma-1}{\gamma}} - 1 \tag{3b}$$

Since the flow is choked at both points 4 and 4',

$$\frac{p_4}{P_4} = \frac{p_4'}{P_4'}$$

But, since $S_4' < S_4$, then $P_4' > P_4$, and hence $p_4' > p_4$. Also, $p_6 = p_6'$ $(= p_0)$ so that, from equations (3a) and (3b),

$$\left(\frac{C}{D}\right)_{4'} > \left(\frac{C}{D}\right)_4$$

Also, a comparison of two similar strips at the start of combustion (in the vicinity of points 0 and 1) shows that

$$\left(\frac{C}{D}\right)_1 > \left(\frac{C}{D}\right)_0$$

inasmuch as $(C/D)_0$ is zero.

The C/D ratio and hence the thermal efficiency thus have been proved greater for both the first and the last increments of heat added in the case of the cycle employing diffusion. It is then argued, although without proof, that all the heat is added more efficiently in the cycle employing diffusion.

It is recognized, however, that, for large amounts of diffusion, the inlet and exit losses have a proportionately greater effect as the work tends toward zero; and so the efficiency must also approach zero. This implies that, for best efficiency, the flow should be diffused to the lowest value of combustor-inlet Mach number that will permit addition of the desired amount of heat; that is, the combustor-inlet Mach number should be lowered until the exit flow is choked. (Numerical calculations are presented in later sections to demonstrate, for specific cases of interest, the validity of the deductions stated in this section on theory.)

Variable combustor area. - To avoid the limitations on heat addition due to choking in a constant-area duct, a variable-area duct may be considered. In figure 3, combustion is initiated at point 1, and path 1-a-4 is followed for a constant-area duct. A Rayleigh line for some larger area duct is also shown, with the choking point at 4'. If a diverging-area duct is employed, the combustion process will follow path 1-4'. The actual shape of the path is dependent on the rate of heat release and the wall contour.

Normal shocks. - Up to this point, it has been assumed that the heat may be added uniformly with no discontinuities of flow. However, the heat release possibly may trigger a normal shock. A shock might occur at the combustor entrance, path 1-1' (fig. 3); combustion would then take place subsonically from 1'-4. Or, the shock might be within the combustor with supersonic burning from 1-a, a normal shock from a-b, and subsonic burning from b-4. In each of these cases, choking would occur at point 4 after the same amount of heat was added; and the same amount of cycle work would be produced. If the normal shock could not be avoided, further subsonic diffusion of the air would be desirable. The cycle would then follow path 0-1-1'-2'-4', which corresponds to a conventional ramjet (CRJ).

Comparison of SCRJ and CRJ. - A comparison of an SCRJ and a CRJ is illustrated in figure 4. Both total and static temperatures are plotted against entropy. Each engine is assumed to undergo the same amount of supersonic diffusion from 0-1. The SCRJ begins the combustion process along 1-P-4. The CRJ goes through a normal shock 1-1' followed by subsonic diffusion 1'-2' and then burns along 2'-Q-4'. Examination of the areas under the Rayleigh lines shows that more heat may be added for a given increment of entropy for the CRJ. Heat addition may also be indicated by an increase in total temperature; hence it follows that the slope of the total-temperature curve is greater in the CRJ case. Therefore, the total-temperature curves for the CRJ and the SCRJ intersect at conditions Q and P, respectively. If the amount of heat added is such that the combustor-exit total temperature is equal to T_p, both the SCRJ and CRJ engines will deliver the same thrust and have the same over-all efficiency (assuming equally efficient exhaust nozzles). For exit total temperatures less than T_p, the SCRJ has the smaller entropy increase, hence the higher total pressure entering the nozzle and hence the higher thrust. This situation may arise when the maximum cycle temperature is limited because of structural reasons or because the fuel-air ratio is stoichiometric. For temperatures higher than T_p, the CRJ is best.

If the SCRJ suffers a normal shock (1-1'), note that the entropy increase is the highest in this case for any value of exit total temperature. Therefore, as previously mentioned, the SCRJ with a normal shock

yields the poorest performance. (However, in the important case where enough heat is added to choke the flow, the same SCRJ performance is obtained with or without a normal shock.)

Method

Thermodynamic assumptions. - The calculations were performed by using the equations of state and conservation of mass, momentum, and energy; one-dimensional flow was assumed. Preliminary calculations were made for an ideal gas having a γ of 1.4. More extensive real-gas calculations were based on the use of hydrogen fuel. The tables of reference 3 were used to account for variable specific heats, but dissociation generally was ignored.

Form of results. - Cycle performance is generally given in terms of the net thrust per unit airflow rate F/w_a and the over-all engine efficiency η_e, where

$$\eta_e = \frac{(F/w_a)V_0\eta_c}{c_p(T_4 - T_2)} = \frac{(F/w_a)V_0}{(f/a)\ H} = \frac{3600}{sfc}\frac{V_0}{H} \tag{4}$$

Both F/w_a and η_e are independent of the particular fuel being used except for the usually minor effect of different gas properties of the combustion products.

Configuration. - Figure 5 illustrates the ramjet configurations. A schematic diagram of an SCRJ is shown in figure 5(a). An inlet diffuser is pictured, but the Mach number at the combustor inlet (station 2) is still supersonic. The flow area at the combustor exit (station 4) may be greater than at the combustor inlet. If no normal shock occurs in the engine, the Mach number at station 4 is no less than 1, so no nozzle throat is required. The flow is expanded through a diverging nozzle exhausting to the atmosphere at station 6.

For comparison, a CRJ is sketched in figure 5(b). Supersonic diffusion takes place from stations 0 to 1 and is followed by a normal shock and further subsonic diffusion from 1' to 2. In the general case, the combustor-exit Mach number is subsonic, and a nozzle throat is needed (station 5).

Heat-transfer. - In order to estimate combustor cooling loads, the convective heat-transfer rate was calculated by using a method proposed by Van Driest (given in ref. 4). This procedure is valid only for the case of no pressure gradient - a condition not obtained in the SCRJ. However, the calculations were not made to obtain absolute values of heat-transfer rates but rather to provide a gross comparison of subsonic and

supersonic burning. The assumptions are believed to be adequate for this purpose.

Weight. - Estimates of engine weights were made in order to compare the SCRJ and CRJ engines.

Component Assumptions

Inlet. - Three types of inlets were considered for the SCRJ:

(1) Wedge type (fig. 5(a)): Air is deflected and compressed by the oblique shock off a wedge of semiangle λ and is turned back to the horizontal by another oblique shock off the cowl lip.

(2) Pitot type (fig. 6(a)): Air enters the combustor at the flight Mach number; this case is treated in the discussion as a special case of the wedge type with $\lambda = 0$.

(3) Isentropic type (fig. 6(b)): Air is isentropically compressed in some unspecified manner to a lower supersonic Mach number before entering the combustor.

The assumed pressure recovery and combustor-inlet Mach number are given in figure 7(a) for the wedge inlets. These values were calculated with a γ of 1.4 and so do not correspond exactly at the higher speeds to the performance of an actual wedge of angle λ in a real gas. The CRJ used for comparison in the present report is assumed to have the pressure recoveries shown in figure 7(b). These values are representative of a two-cone external-compression inlet (ref. 5).

Combustion chamber. - In the absence of conclusive experimental justification, stable supersonic combustion is assumed possible for any combustor-inlet Mach number and fuel-air ratio. For the CRJ, a combustor-inlet Mach number of 0.175 was used; the results are insensitive to changes from this value. The combustion efficiency was taken as 0.95 for both the SCRJ and the CRJ.

The momentum pressure drop due to heat addition was calculated in each case. No slowing down of the combustor flow due to the injection of fuel was assumed in most of the calculations. This is approximately equivalent to assuming that the fuel is injected axially at the velocity existing at the combustor exit. (This requirement is easily achieved because of the high acoustic velocity of hydrogen.) Separate calculations were also made to indicate the effect of nonaxial mass addition.

Exhaust nozzle. - The combustion products generally were considered to be fully expanded to ambient pressure with a velocity coefficient of 0.96. The effects of varying these assumptions were investigated.

RESULTS AND DISCUSSION

The previously presented section on theory attempted to indicate some of the significant features of the SCRJ by discussion of the temperature-entropy diagram. The actual results of the numerical calculations are presented in this part of the report and apply to any altitude in the isothermal region of the atmosphere. Results of the real-gas calculations (that is, with variable specific heats) are generally given in terms of absolute values. Results of the ideal-gas calculations are valid for the trends found and are given in terms of ratios to some standard condition.

The first part of this section discusses the major-cycle parameters (combustion temperature, inlet type, flight Mach number) and compares the SCRJ and CRJ. The second part discusses the effects of other cycle parameters (nozzle performance, diverging combustors, wall friction) and also considers additional factors, such as cooling loads and engine weight.

Major-Cycle Parameters

All data herein are given for a constant-area combustor having no wall friction and a fully expanded exhaust nozzle with a velocity coefficient of 0.96.

Effect of combustion temperature. - Figure 8 shows η_e and F/w_a for an SCRJ at $M_0 = 6$ as a function of the combustor-exit total temperature T_4 for two different amounts of supersonic diffusion. The solid lines in figure 8 were constructed with the assumption that the heat addition had caused a normal shock at some point upstream of the combustor exit, the exact location being immaterial; the combustor-exit Mach number is therefore subsonic. The dashed lines in this figure correspond to the case of shock-free supersonic flow throughout the engine. The different amounts of diffusion were obtained by employing 5- and 10-degree wedge inlets.

Figure 8 shows that higher thrust and efficiency are obtained without the occurrence of the normal shock. The explanation for this is similar to the previously given discussion of figure 4.

Figure 8 also indicates that the difference in engine performance with and without the normal shock diminishes as the amount of heat added is increased. At the limiting condition, with the flow choked at the combustor exit, the thrust and efficiency are the same with and without the shock. Also, the values of thrust and efficiency are approximately maximum at this point. Therefore, from a cycle viewpoint, it seems desirable to add sufficient heat to choke the flow. However, the choked-flow combustion temperature may not always be attainable because of encountering

stoichiometric fuel-air ratios (or engine structural limitations) before choking occurs. There is no fuel restriction in figure 8, since the stoichiometric combustion temperature at Mach 6 is about 6000° R. However, these limitations become more restrictive as the flight speed is increased.

Figure 9 shows the difference in the effect of T_4 on the performance of the SCRJ and CRJ. In figure 9, the over-all engine total-pressure ratio (P_4/P_0) and the over-all engine efficiency are plotted as functions of T_4. The use of P_4/P_0 has the advantage of showing the combined effects of inlet and combustion total-pressure losses; it is in the distribution of total-pressure losses between these two components that the CRJ and SCRJ differ. Because of the very low value of M_2, the total-pressure loss involved in the entire CRJ cycle is largely due to the inlet and varies only slightly with the heat addition. Conversely, the SCRJ with no normal shock in the inlet will always have less inlet total-pressure loss, and much higher combustion loss due to the higher value of M_2. Therefore, the SCRJ starts initially with a high value of P_4/P_0 that decreases rapidly with increasing temperature. As indicated in the figure, the two curves eventually intersect unless terminated first by choking. The point of intersection, then, depends on the magnitude of the difference in inlet performance and on the value of M_2. Since the heat addition is the same for each engine at any given value of T_4, the engine with the highest total pressure at the end of combustion will be able to produce more thrust and therefore have the highest efficiency (assuming the same value of C_V for each engine). Therefore, as illustrated in figure 9, the intersections of the efficiency and P_4/P_0 curves occur at the same value of T_4.

The efficiency curves in the lower half of figure 9 show an additional difference between the SCRJ and the CRJ cycles. The CRJ displays a definite maximum in efficiency, whereas the SCRJ chokes before a clearly defined maximum occurs.

Because of the apparent advantages of choking the flow in the SCRJ combustor, all the following results are for this condition unless otherwise stated.

Effects of supersonic diffusion. - In the Theory section, it was pointed out that the SCRJ cycle may benefit from the use of a diffuser to raise the pressure of the air entering the combustor.

Figure 10 gives the effect of varying amounts of supersonic diffusion with a wedge inlet. More diffusion lowers the combustor-inlet Mach number towards 1, so that less heat may be added before choking occurs in the constant-area duct. Hence the combustion temperature is considerably

reduced as the wedge angle is increased. The reduced amount of heat addition lowers the pressure rise experienced in the combustion chamber; however, the pressure rise through the diffuser is large enough so that a net rise in combustor-exit pressure occurs with larger wedge angles. Because of the increased nozzle pressure ratio, the thrust initially increases with increasing wedge angle despite the falling combustion temperature. Eventually, however, the amount of heat that may be added is so limited that the cycle work begins to decrease. Consequently, there is an optimum wedge angle for maximum thrust.

For low amounts of diffusion, with the thrust increasing and the heat added decreasing, the over-all engine efficiency increases rapidly with increasing wedge angle. At the angle where the thrust is a maximum (7° for the case shown), the heat addition is still decreasing. Consequently, the efficiency continues to improve and reaches a maximum at a much higher angle (13°).

For a flight Mach number of 6, improvements (over the Pitot inlet) in either thrust or over-all efficiency of 23 or 61 percent, respectively, are possible by using the properly chosen wedge inlet. Similar gains may be realized at other flight conditions. Gains of this magnitude probably justify the additional complexity of the wedge as opposed to the simple Pitot inlet.

The wedge inlet imposes significant total-pressure losses as the air traverses the two oblique shocks (see fig. 7(a)). More sophisticated inlet designs, which afford improved pressure recoveries, are available, although at the expense of increased complexity and sensitivity to operating conditions. To indicate the further gains possible with more refined inlets, figure 11 presents the performance attainable with a perfect inlet; that is, the air is isentropically decelerated to any desired supersonic combustor-inlet Mach number. So-called isentropic inlets, when applied to the CRJ, still have appreciable pressure losses. Such losses are usually attributable to turning losses, boundary-layer separation, and a necessary normal shock for stabilization in the vicinity of the inlet throat as the flow decelerates through Mach 1. Since, however, the SCRJ diffuser maintains the air supersonic throughout, there is some hope that such throat losses may be avoided in a properly designed inlet and that the deceleration process will be nearly isentropic.

As for the wedge inlets, figure 11 shows that more diffusion is required for maximum efficiency than for maximum thrust. For the two flight speeds shown, the maximum efficiency is achieved when the air is decelerated to a Mach number of about 2.5. This was also found to be true for all flight Mach numbers between 4 and 7.

Comparison of SCRJ and CRJ. - Figure 12 presents the maximum over-all engine efficiency at various flight speeds for SCRJ and CRJ cycles with different inlet types.

Efficiency increases with flight Mach number for all engines in the speed range shown. Performance of the SCRJ with Pitot inlet is quite poor. A major improvement is achieved with the use of a wedge inlet. Smaller, though significant, further improvement is provided for the SCRJ if isentropic diffusion is possible.

When compared with the CRJ (with two-cone inlet), the SCRJ provides better engine efficiency at flight Mach numbers above 7 if a wedge inlet is used or above 5 if an isentropic inlet is used. For comparative purposes, figure 12 also shows a curve for the CRJ performance with an ideal inlet. This case has negligible inlet and combustor pressure losses and thus represents an ultimate limit in ramjet performance. The figure indicates that the SCRJ does not fall very far short of this goal at high Mach numbers if isentropic diffusion can be realized.

Secondary-Cycle Parameters

The previous section discussed the major-cycle parameters. The SCRJ engine is also affected by a number of other factors, which are presented herein. These factors include the effects of fuel injection, nozzle velocity coefficient and expansion ratio, combustor area variation and wall friction, engine cooling loads, and engine weight.

Effects of mass addition. - The injection of a fluid such as fuel into a supersonic airstream may cause oblique shocks to form around the points of injection or even around the drops of fluid if injected as a liquid. The severity of such shocks is not known, and no losses due to this effect have been assumed in the analysis.

Another effect, which cannot be ignored, is the momentum interchange between the fluid and the air if the fluid is injected at zero axial velocity and if a uniform mixture is assumed to exist at the combustor exit. To illustrate this effect, engine performance is presented in figure 13 for arbitrary values of m/a, the weight ratio of injected fluid to air. The fluid is assumed to be injected normal to the airflow direction, and no change in specific heat or gas constant is assumed through the combustor. Of course, the injected fluid is usually fuel, and the amount added is set by the desired combustion temperature. Variations in m/a in practice might result from:

(1) Changes in fuel type

(2) Variations in combustion efficiency

(3) Injection of another fluid in addition to fuel

The efficiency parameter shown in figure 13 is the over-all engine efficiency divided by the combustion efficiency, which may be written

$$\frac{\eta_e}{\eta_c} = \frac{V_0(F/w_a)}{Jc_p(T_4 - T_2)}$$

This parameter is independent of the fluid heating value (which changes in cases 1 and 3) and of the combustion efficiency. Therefore, only the direct effect on the cycle of mass addition is shown.

Figure 13 shows that increasing the mass addition causes a large decrease in thrust. The additional mass decelerates the airflow, and so less heat may be added before the choking limit is encountered; thus, the thrust is reduced. However, the amount of heat addition decreases faster than the thrust. Therefore, as shown, the efficiency parameter η_e/η_c does not decrease in direct proportion to the thrust (as is the case with the CRJ); in fact, η_e/η_c increases. There is, of course, no net benefit from this improvement. The increase in m/a arises fundamentally because of a reduction in either η_c or fuel heating value, both of which tend to increase engine fuel consumption. However, the rise in η_e/η_c does act to counteract this effect somewhat.

The large decrease in thrust for the SCRJ is in contrast to the CRJ. For the latter engine, the momentum interchange between the subsonic airflow and the injected fluid is small, the thrust is not usually limited by choking, and the increased mass of the exhaust gas yields an increase in thrust as m/a is increased.

A Pitot inlet was assumed in figure 13. An engine employing supersonic diffusion would not have such high combustor velocities and thus would not suffer such large thrust losses due to mass addition.

In the other sections of this report, the fuel is assumed to be added with a great enough axial velocity that there are no losses due to the momentum interchange just described.

Effect of nozzle velocity coefficient. - The preceding results are based on a velocity coefficient of 0.96. Figure 14 indicates the sensitivity of engine performance to variations in this value. Thrust and over-all efficiency, normalized with respect to their values at a C_V of 1.0, are given. Since changes in velocity coefficient do not affect the combustor heat addition, the thrust and efficiency vary in the same proportion.

The sensitivity to changes in velocity coefficient decreases with higher flight Mach number. But even at the highest speed shown, a

1-percent decrease in C_V causes a 5-percent loss in both thrust and engine efficiency. It is therefore essential to achieve high nozzle efficiencies.

As shown in figure 8, best engine performance is achieved when the combustor exit is choked. The exhaust nozzle will, therefore, generally not require a convergent section; this may tend to improve the velocity coefficient somewhat. On the other hand, the nozzle pressure ratios are in the order of several hundred, which will make it difficult to achieve efficient expansion. For this reason a velocity coefficient of 0.96 has been used throughout this study. Although higher values are generally quoted for well-designed convergent-divergent nozzles, little experimental work has been done in this pressure range.

Effect of nozzle expansion ratio. - The nozzles in the present study are generally assumed to completely expand the combustion gas to ambient pressure. Since the nozzle pressure ratios are usually in the order of several hundred, very large nozzles are required. In some cases, the exit area may be more than 20 times greater than the combustor area. To reduce the weight and external drag penalties associated with such large nozzles, decreasing the nozzle-exit area is desirable.

The effect of the consequent underexpansion on internal engine performance is given in figure 15. Two cases are presented in terms of thrust or over-all efficiency relative to their values at the fully expanding condition. The velocity coefficient is held constant at 0.96, although some improvement would be expected as the nozzle size is reduced.

For nozzles that are only slightly underexpanded, the thrust increment produced by the excess pressure acting on the exit area approaches the thrust increment due to the extra velocity that could be realized by expanding that pressure through a perfect nozzle. In a real nozzle, however, the velocity coefficient is also applied to that last increment of velocity, so that the thrust increment is decreased by a constant fraction. Therefore, as shown in figure 15, the cycle thrust and over-all efficiency are improved by moderate amounts of underexpansion. For the engine with an isentropic inlet, the exit area may be reduced by 50 percent without harming the cycle performance. Similar, though smaller, reductions in area may be made for the lower-performance Pitot-type engine.

It is concluded that actual SCRJ engines should be designed with underexpanding exhaust nozzles, since savings in weight and drag can be made with little penalty to internal performance.

Effect of combustor area variation. - As noted previously, both the thrust and over-all efficiency increase with increasing combustion temperature until the limit of thermal choking is encountered at the exit

of the constant-area combustor. Enlarging the combustor exit would raise the choking temperature with the possibility of yielding still higher thrusts and efficiencies due to the increased heat addition. A more physical interpretation is that the diverging combustor walls would experience a component of force in the axial direction and so add to the thrust.

The thrust produced will be dependent on the axial distributions of pressure and diameter through the combustor. An effective average pressure $\overline{p}$ may be visualized to act on the total projected wall area $A_4 - A_2$. For any reasonable wall contour, the effective pressure has a value between the inlet and exit pressure and may be conveniently expressed in terms of a factor n such that

$$\left.\begin{aligned} \overline{p} &= p_2 + n(p_4 - p_2) \\ \text{or} \\ n &= \frac{\overline{p} - p_2}{p_4 - p_2} \end{aligned}\right\} \qquad (5)$$

where n is a number between 0 and 1. Inserting the wall force $\overline{p}(A_4 - A_2)$ into the usual large-scale, one-dimensional momentum equation readily permits a solution for the combustor momentum-pressure drop. The engine thrust and efficiency may then be computed in the usual way. Some typical results are presented in figure 16 for various combustor area ratios with n as an arbitrary parameter.

The figure shows the obvious result that high values of n (i.e., high $\overline{p}$) are desirable. If n is sufficiently high, increasing the combustor area ratio is beneficial to the thrust and, to a lesser extent, to the over-all efficiency. As the area ratio is increased, more heat is required to choke the flow. The curves in figure 16 have been ended at approximately the stoichiometric fuel-air ratio.

Figure 16 emphasizes that the engine performance with a diverging combustor is sensitive to variations in n. It is therefore desirable to determine what values of n can be achieved in practice. No convenient analytical means of predicting n appears available. Therefore, to obtain at least some insight into the problem, the following approach was adopted. First, the area distribution was fixed by assuming that the combustor is conical. Second, various pressure distributions were arbitrarily assumed. From these distributions, values of $\overline{p}$ and n were calculated. The assumed pressure distributions are pictured in figure 17(a) and the corresponding axial temperature distributions in figure 17(b). These distributions are of no particular significance other than that they represent more or less reasonable guesses as to what might exist in an actual combustor.

The resultant values of n are plotted against area ratio in figure 18. Appreciably different values, depending on the distribution and, in one case, on the area ratio, are obtained. In the absence of any firm indication as to a proper value, n was taken as 0.5 in all succeeding calculations involving a diverging combustor.

Figure 19 illustrates typical engine performance as a function of A_4/A_2 for wedge and isentropic inlets (figs. 19(a) and (b), respectively). Increasing the area ratio substantially improves F/w_a. The over-all efficiency is generally insensitive to changes in A_4/A_2. An exception occurs when the heat addition is extremely limited in a constant-area combustor. Thus, in figure 19(b), the thrust is very low for the case of a flight Mach number of 4.0 and a combustor-inlet Mach number of 2.0, when the area ratio is 1.0. Internal losses have a large effect in this low-thrust condition (i.e., they are a large portion of the net thrust), and the over-all efficiency is poor. Increasing the area ratio, producing greater thrust, is then also beneficial to the efficiency. Thus, for this case, the optimum A_4/A_2 improves the efficiency from 0.34 to 0.42.

As the combustor area divergence is increased, F/w_a is generally improved. The thrust per unit frontal area does not necessarily vary in the same manner, however; this depends on which area is used as a reference. This situation is indicated in figure 20. The inlet lip area does not vary with A_4/A_2 and so the thrust coefficient based on lip area $C_{F,0}$ increases in the same ratio as F/w_a. On the other hand, A_4 increases directly with A_4/A_2. The resulting thrust coefficient based on A_4 is nearly constant and, in fact, displays a slight maximum. The nozzle-exit area A_6 also increases with A_4 but not as rapidly, since the greater pressure losses associated with increased A_4 reduce the nozzle expansion ratio. Therefore, $C_{F,6}$ increases with A_4/A_2. These various thrust coefficients are of interest as indications of engine weight, volume, or nacelle drag per unit thrust.

Effect of wall friction. - The preceding discussion has ignored the effects of combustor wall friction on the engine performance. Because of the high flow velocities in the SCRJ, significant friction losses might be expected. The friction drag at each point in the combustor will depend on the local flow conditions and consequently is affected by the axial distribution of temperature and pressure.

For some axial distributions, the differential equations of flow can be integrated directly. This has been done for distributions 1 and 2 (fig. 17(a)), considered in the preceding section on variable-area combustors. For simplicity, the combustor area and the local drag coefficient were assumed constant. Typical resulting engine performance is

shown in figure 21, where the thrust and over-all efficiency (relative to the no-drag condition) are plotted against the product of the friction drag coefficient and the combustor length-diameter ratio. An alternative large-scale solution to the combustor process is also shown in figure 21. In this method, an effective, constant wall-shearing stress was assumed equal to the product of the friction drag coefficient and the dynamic pressure at the combustor inlet. A direct solution for the combustor is possible in this case without the need for integrating. Figure 21 indicates that the two methods give very similar results. Therefore, the less complicated large-scale approach was employed in the subsequent calculations.

The effect of friction at several different flight speeds is given in figure 22. Large friction losses are seen to produce the greatest effect at low flight speeds where any loss becomes an important part of the total engine output. The importance of the friction drag will depend critically on the combustor length needed for efficient combustion. For example, a representative value of drag coefficient is 0.0025. If the combustor length-diameter ratio were 3, then the thrust and over-all efficiency at a Mach number of 6 would be 14 and 8 percent, respectively, less than the no-drag values. If a length-diameter ratio of 6 were required, these losses would be approximately doubled.

It is seen, therefore, that the SCRJ may be significantly penalized by internal wall friction. However, figures 21 and 22 consider only the Pitot-type inlet. Engines using the higher performance inlets would not be as sensitive to friction losses.

Combustor cooling load. - Because of the unusual combustor flow conditions, the SCRJ may be expected to encounter different cooling problems than the CRJ. As a partial indication of these differences, the local convective heat-transfer rate was calculated for two identical combustors, one with supersonic velocities throughout and the other with a normal shock at the inlet followed by subsonic velocities.

The method of reference 4, which is for turbulent flow over a flat plate with no pressure gradient, was used. The gas was assumed to be air, with the transport properties taken from reference 6. This method does not really apply to the supersonic combustor, which has a large adverse pressure gradient; however, it was felt to be adequate for purposes of qualitative comparison.

Figure 23 shows the calculated local convective heat load through the combustor if the walls are held at a temperature of 1200° R. The data are based on a 5-foot length and a sinusoidal axial pressure variation. A Pitot inlet is specified in order to obtain the maximum value of combustor-inlet Mach number for the supersonic case (i.e., equal to flight Mach number). The same inlet is used for the subsonic case. The

heat-transfer rate is greatest in the case of subsonic combustion, as a result of the higher temperatures and pressures after the normal shock. The average heat-transfer rate is 19 percent higher than for the supersonic case at a Mach number of 4, and 29 percent higher at Mach 6. If a more efficient diffuser were used for the subsonic case, the pressures and hence the heat-transfer rate would be still higher. Although not shown in figure 23, the radiative heat-transfer rate, being a function mainly of temperature, would also be higher for the subsonic case.

Thus, for the same amount of heat addition, the SCRJ has lower local heat-transfer rates than the CRJ. On the other hand, the SCRJ may have more combustor surface area because of both narrower flow passages and a longer combustor. Therefore, the total cooling load may not be reduced in the same proportion as the local heat-transfer rate.

Effect of dissociation and frozen expansion. - At high flight speeds, the optimum combustion temperature in a ramjet is high enough to appreciably dissociate the combustion products. During an equilibrium nozzle expansion process, the temperature drops and the gases reassociate. In some cases, however, insufficient residence time is available for reassociation, and the gas composition remains frozen throughout the expansion. Such failure to recover the energy of dissociation is deleterious to the performance of the engine.

For any given amount of heat addition, the SCRJ will have lower combustor static temperatures than the CRJ. Since less dissociation then occurs, any possible losses due to frozen nozzle expansion are reduced. This situation is illustrated in figure 24, where the engine thrust is compared for both equilibrium and frozen expansion at an altitude of 120,000 feet.

For the flight conditions presented in the equilibrium case the SCRJ is slightly superior at low combustor total temperatures but is poorer at the higher temperatures. Because of the low combustor static temperatures, however, the SCRJ suffers little losses if frozen expansion occurs. On the other hand, the static temperatures in the CRJ are very near the total temperature. Appreciable dissociation is present in the entire range of total temperatures shown, and there are substantial thrust losses if frozen expansion occurs. As a result, the SCRJ is found to provide higher thrust than the CRJ over the entire range of total temperatures if recombination does not take place.

A similar situation may occur if boron-containing fuels are employed. One of the combustion products is boric oxide (B_2O_3), which is a vapor at the high temperatures present in the combustion chamber, but which condenses at temperatures in the order of 2500° R. Failure of the B_2O_3 to condense during the expansion leads to the same type of engine losses that occur when the dissociated gases fail to recombine. The lower static

temperatures in the SCRJ are again an advantage because they reduce the amount of vaporized B_2O_3 entering the nozzle.

Comparison of engine weights. - Having no subsonic inlet diffuser, the SCRJ may be expected to exhibit a weight advantage over the CRJ. On the other hand, the combustor of the SCRJ may be longer and thus heavier. In order to make gross comparisons, simplified weight estimates were made and are presented in table I. The principal assumptions are: (1) The centerbodies of both engine types contain so much useful volume that they are charged to the airframe structure and are not included in the engine weight; (2) the combustor length is 6 feet for the CRJ and 12 feet for the SCRJ; and (3) the engines are considered to have circular cross sections with an inlet diameter of 4 feet.

The table shows that the CRJ has approximately the same weight per unit lip area (or per unit airflow) as the two typical SCRJ engines. Relative to the CRJ, the SCRJ with isentropic inlet has about the same thrust-to-weight ratio. Because of its low maximum thrust, however, the SCRJ with wedge inlet is much poorer.

Although the weight estimates were not precise, it appears reasonable to conclude that the SCRJ offers no weight saving over the CRJ.

CONCLUSIONS

Based on the assumption that shock-free internal burning is possible in a supersonic airstream, calculations were made of the performance of ramjets using supersonic combustion velocities.

With a constant-area combustor, both maximum thrust and over-all engine efficiency are achieved when sufficient heat is released to choke the flow at the exit. In this case, identical cycle performance is attained with and without a normal shock occurring in the combustor. For the same inlet conditions, choking the flow may not be possible because of structural or fuel limitations on the maximum combustor temperature. In these cases, the occurrence of a normal shock does reduce the engine performance, and maintaining shock-free flow is then desirable. However, still better performance generally can be achieved by employing supersonic diffusion, so that choking can be accomplished with the permissible maximum combustion temperature.

In the flight Mach number range considered, from 4 to 7, the over-all engine efficiency of both the supersonic-combustion ramjet (SCRJ) and the conventional ramjet (CRJ) increases with flight speed. The relative merit of these engines depends on the inlet type considered. When compared with a CRJ engine with a two-cone inlet, the SCRJ with a Pitot inlet is less efficient at all flight speeds; with a wedge inlet it is more

efficient above Mach 7; and with an isentropic inlet it is more efficient above Mach 5. At Mach 7, the maximum over-all efficiency is 45 and 54 percent for the wedge and isentropic inlets, respectively.

The thrust and, in some cases, the efficiency of the SCRJ can be improved by using a combustor with increasing flow area. The local heat-transfer rates for the SCRJ combustor are lower than for the CRJ, but the total cooling load may not be less, because of differences in surface area. Performance losses resulting from frozen nozzle expansion are smaller for the SCRJ than for the CRJ in some cases. The SCRJ is very sensitive to changes in nozzle efficiency. Simplified weight estimates do not show any weight advantage for the SCRJ engine, but the results depend on the length of the combustor assumed. If the combustors required for efficient supersonic combustion are long, the wall friction drag becomes substantial.

A number of fundamental problems must be solved before the SCRJ can be considered feasible. The major unknown is whether or not supersonic flow can be maintained during a combustion process. Also, even if a uniform fuel-air mixture can be so burned, there still remains the difficult problem of producing the desired combustible mixtures by fuel injection without causing severe shock losses.

Subject to these qualifications, it is concluded from the present preliminary analysis that the SCRJ does not offer substantial performance gains over the CRJ for flight Mach numbers up to approximately 5 or 7. However, the trends developed herein indicate that the SCRJ will provide superior performance at higher hypersonic flight speeds.

Lewis Flight Propulsion Laboratory
National Advisory Committee for Aeronautics
Cleveland, Ohio, August 20, 1958

REFERENCES

1. Pinkel, I. Irving, Serafini, John S., and Gregg, John L.: Pressure Distribution and Aerodynamic Coefficients Associated with Heat Addition to a Supersonic Air Stream Adjacent to Two-Dimensional Supersonic Wing. NACA RM E51K26, 1952.

2. Dunlap, R., Brehm, R. L., and Nicholls, J. A.: A Preliminary Study of the Application of Steady-State Detonative Combustion to a Reaction Engine. Tech. Note 2284-15-T, Eng. Res. Inst., Univ. Mich., Sept. 1957. (Contract AF 18(600)-1199.)

3. Hall, Eldon W., and Weber, Richard J.: Tables and Charts for Thermodynamic Calculations Involving Air and Fuels Containing Boron, Carbon, Hydrogen, and Oxygen. NACA RM E56B27, 1956.

4. Lee, Dorothy B., and Faget, Maxime A.: Charts Adapted from Van Driest's Turbulent Flat-Plate Theory for Determining Values of Turbulent Aerodynamic Friction and Heat-Transfer Coefficients. NACA TN 3811, 1956.

5. Connors, James F., and Meyer, Rudolph C.: Design Criteria for Axisymmetrical and Two-Dimensional Supersonic Inlets and Exits. NACA TN 3589, 1956.

6. Hilsenrath, Joseph, et al.: Tables of Thermal Properties of Gases. Cir. 564, NBS, Nov. 1, 1955.

TABLE I. - CHARACTERISTICS OF TYPICAL ENGINES

[Flight Mach number, 6.0; design pressure altitude, 60,000 feet]

Engine and inlet type	CRJ (two-cone)	SCRJ (15° wedge)	SCRJ (isentropic)
A_0/A_2	2.45	6.98	13.45
A_4/A_2	1.00	1.00	2.50
A_5/A_4	.50	1.00	1.00
A_6/A_4	11.88	23.56	24.01
t_4, °R	5927	3807	5925
p_2, lb/sq in.	252	28	52
p_4, lb/sq in.	129	147	137
F/w_a	94.25	32.81	92.10
η_e	.446	.420	.451
W_d/A_0, lb/sq ft	13.2	0	0
W_c/A_0	9.3	20.6	22.1
W_s/A_0	54.8	58.1	68.6
W_N/A_0	29.5	15.0	21.9
Total W/A_0, lb/sq ft	106.8	93.7	112.6
Relative F/W, percent	100	40	93

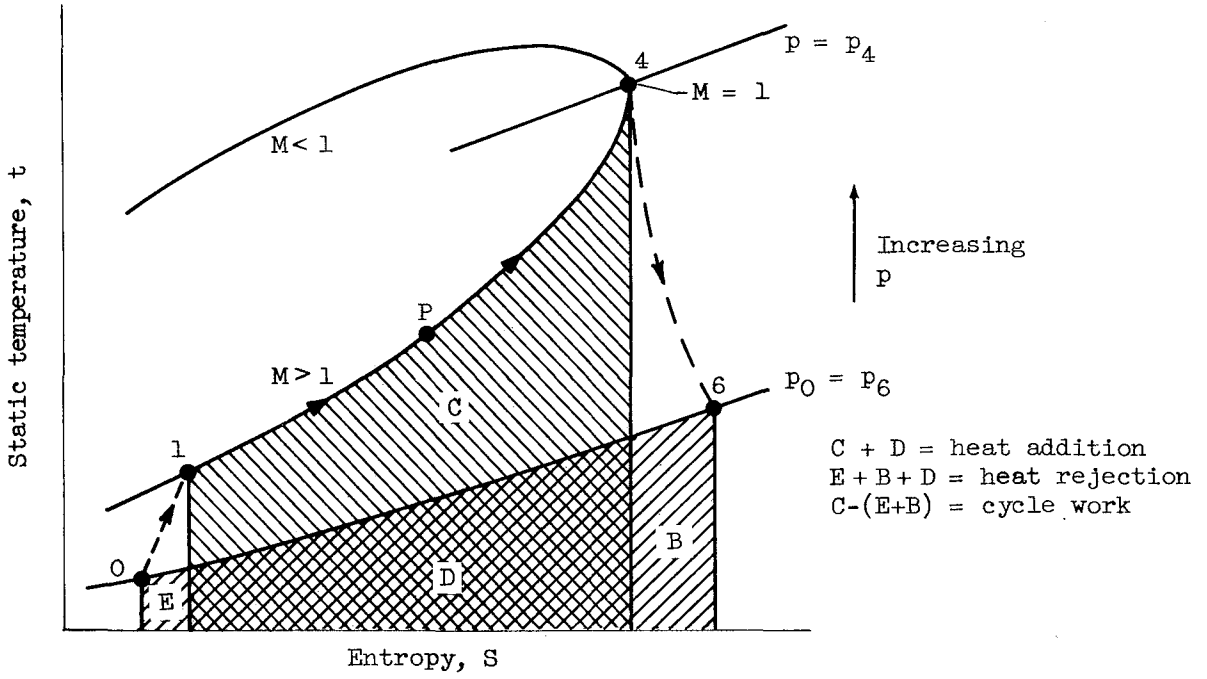

Figure 1. - Temperature-entropy diagram of supersonic-combustion ramjet cycle with inlet and exit losses. Maximum heat addition; constant combustor area.

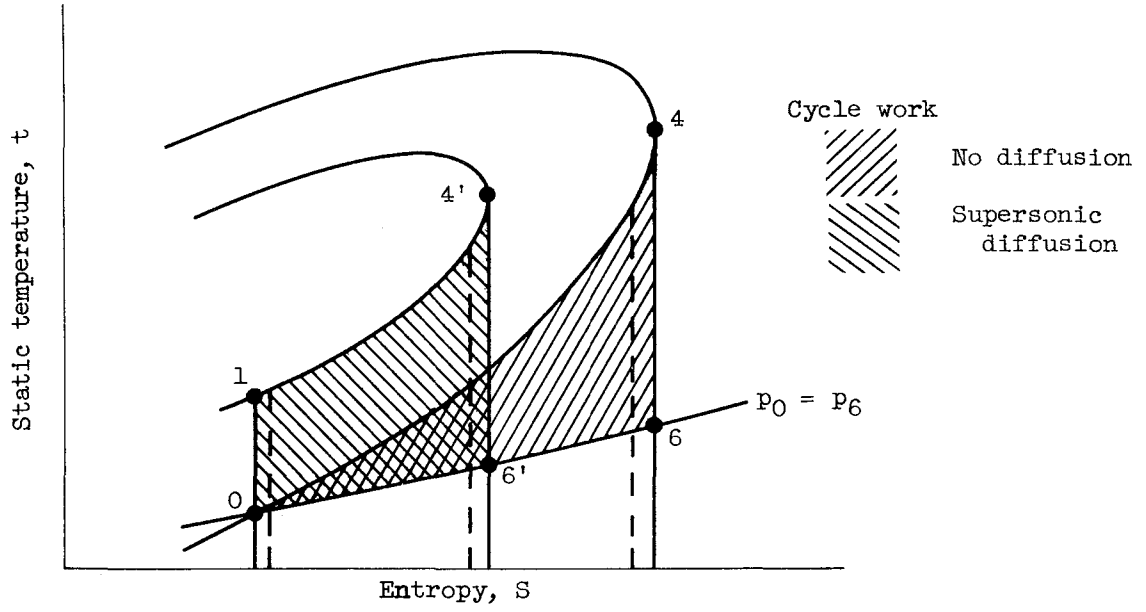

Figure 2. - Temperature-entropy diagram comparing work output with and without supersonic diffusion prior to supersonic combustion. Maximum heat addition; no inlet or exit losses shown.

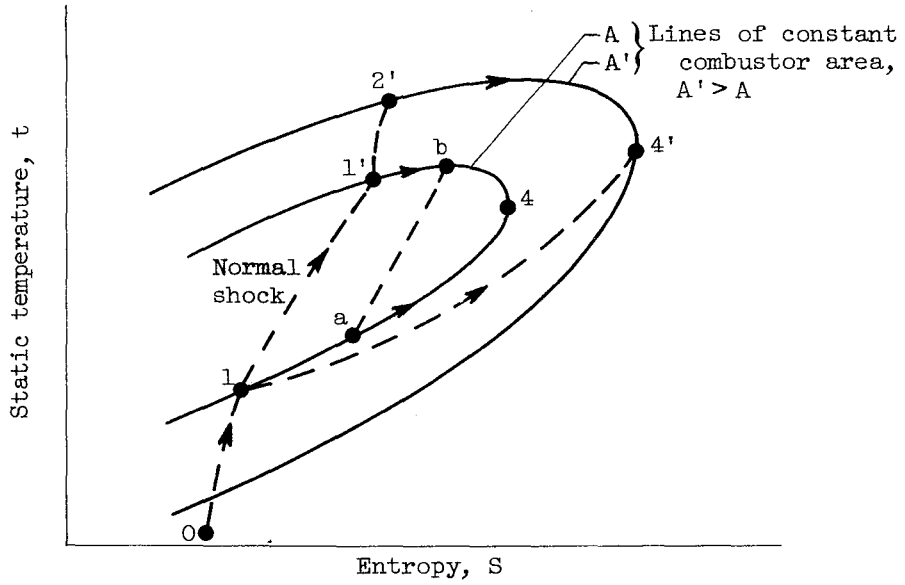

Figure 3. - Combustion with variable combustor area.

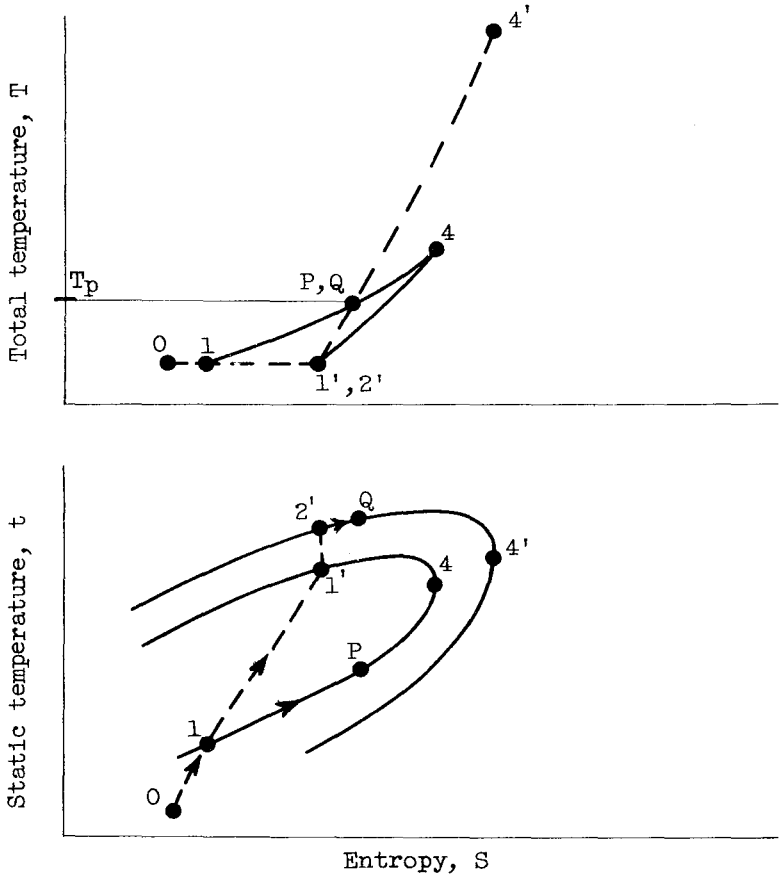

Figure 4. - Comparison of supersonic and conventional ramjet cycles.

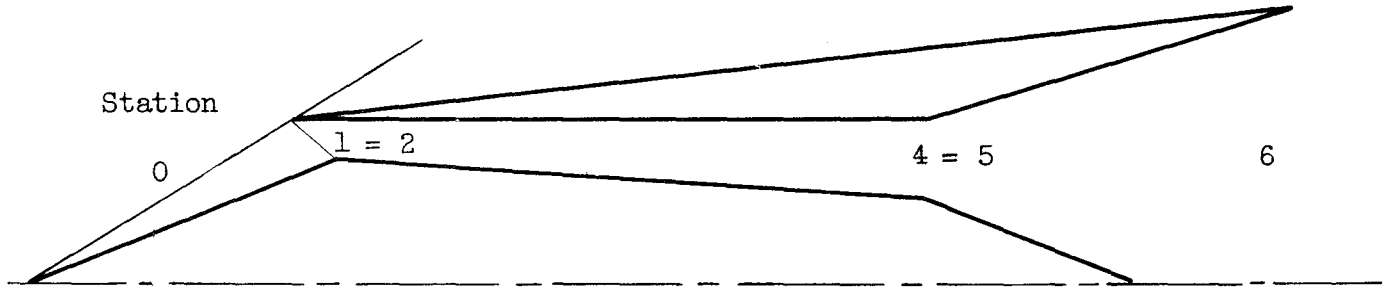

(a) Supersonic-combustion ramjet.

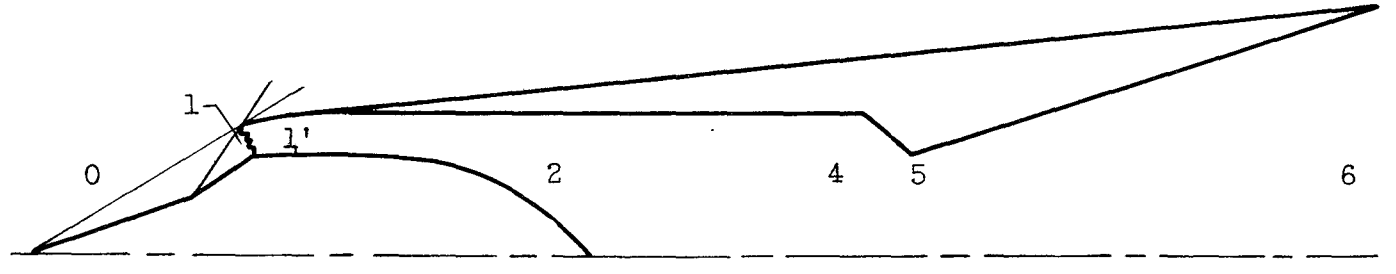

(b) Conventional ramjet.

Figure 5. - Ramjet configurations.

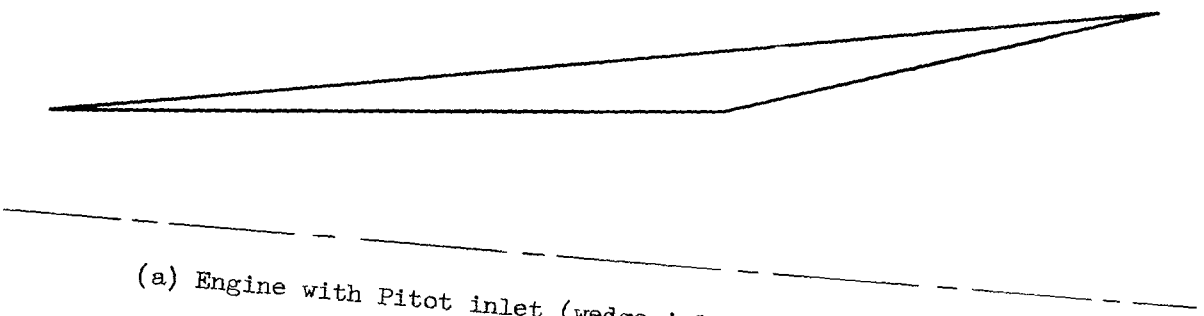

(a) Engine with Pitot inlet (wedge inlet with angle $\lambda = 0$).

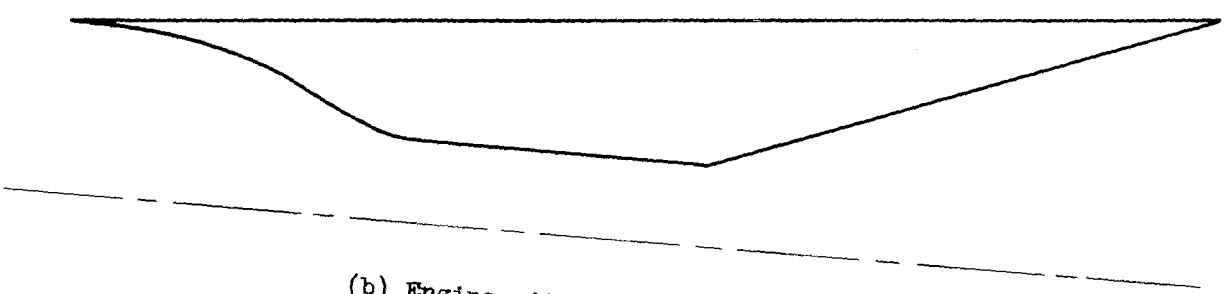

(b) Engine with isentropic inlet.

Figure 6. - Inlet types.

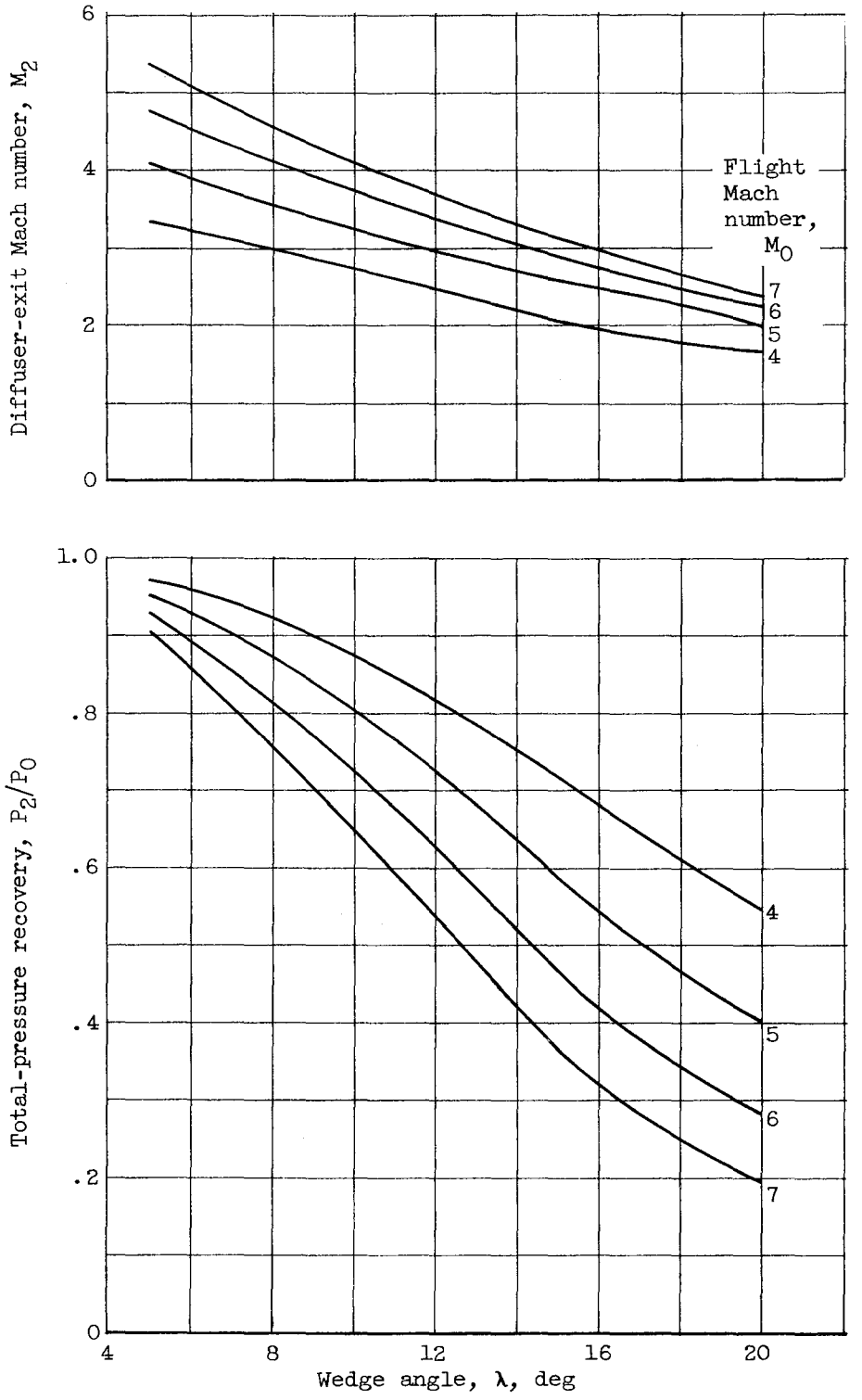

(a) Wedge inlet for SCRJ.

Figure 7. - Assumed performance of inlets.

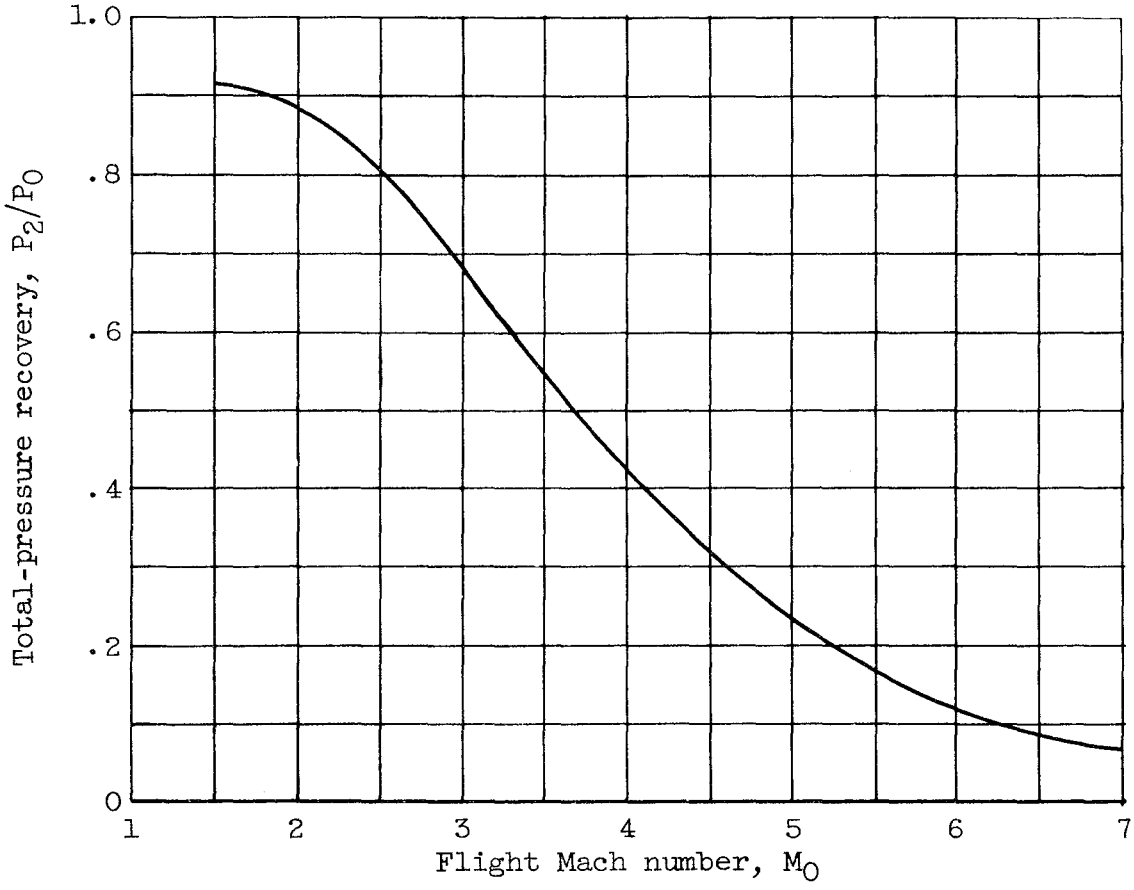

(b) Two-cone inlet for CRJ.

Figure 7. - Concluded. Assumed performance of inlets.

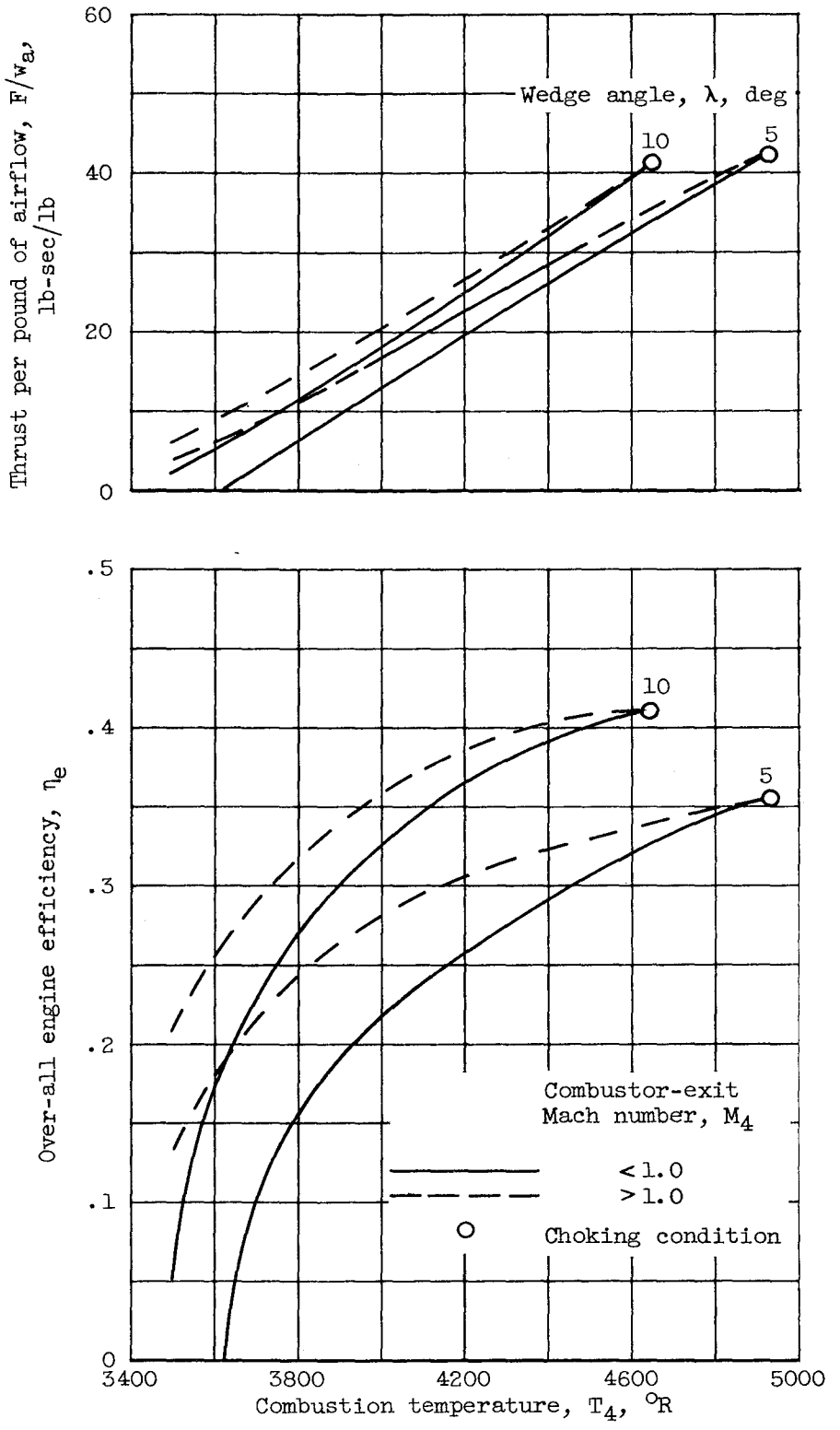

Figure 8. - Effect of combustion temperature on performance of SCRJ. Wedge inlet; M_0, 6.0; A_4/A_2, 1.0; η_c, 0.95; C_V, 0.96; real gas.

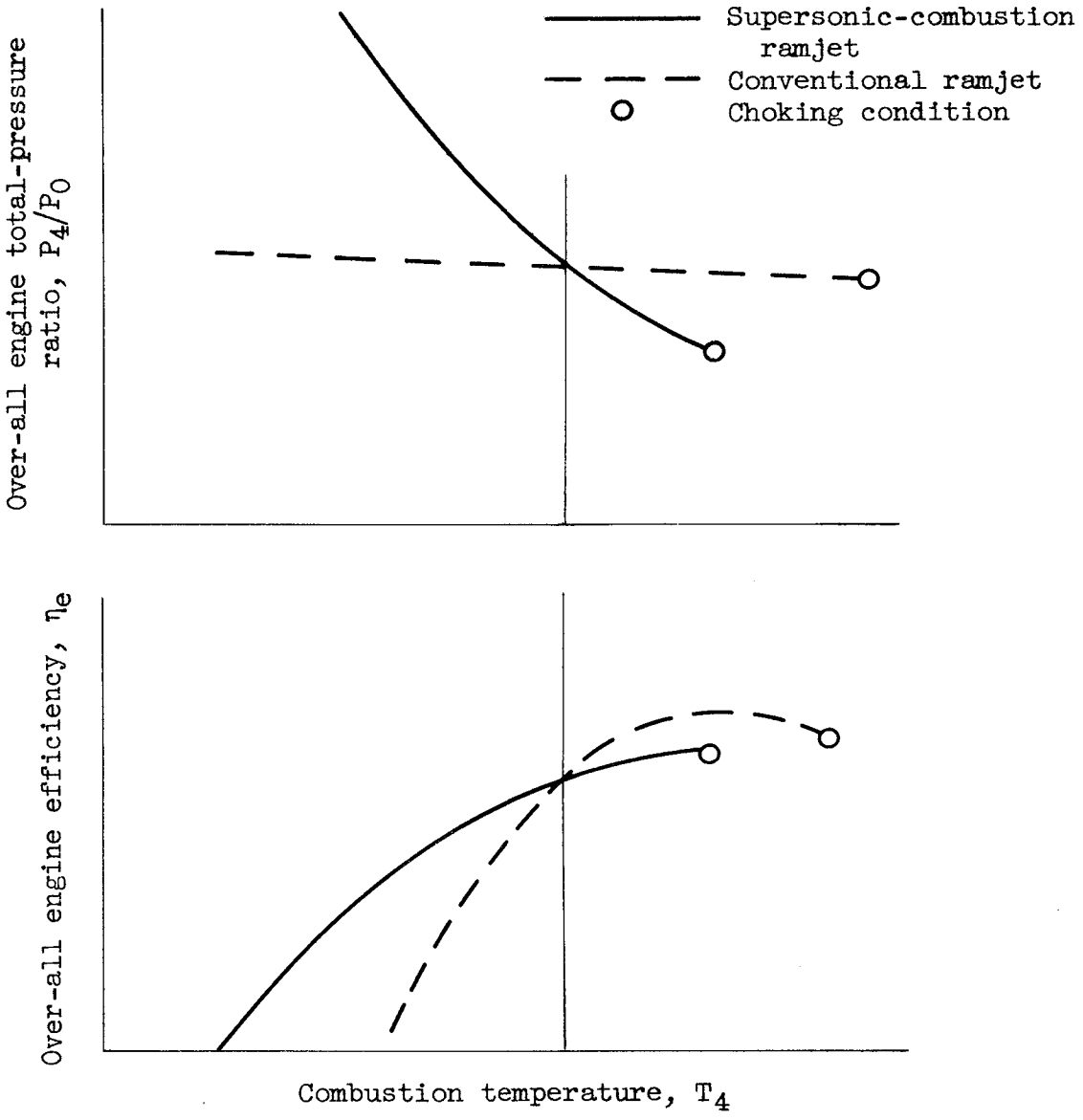

Figure 9. - Effect of combustion temperature on conventional and supersonic-combustion ramjets.

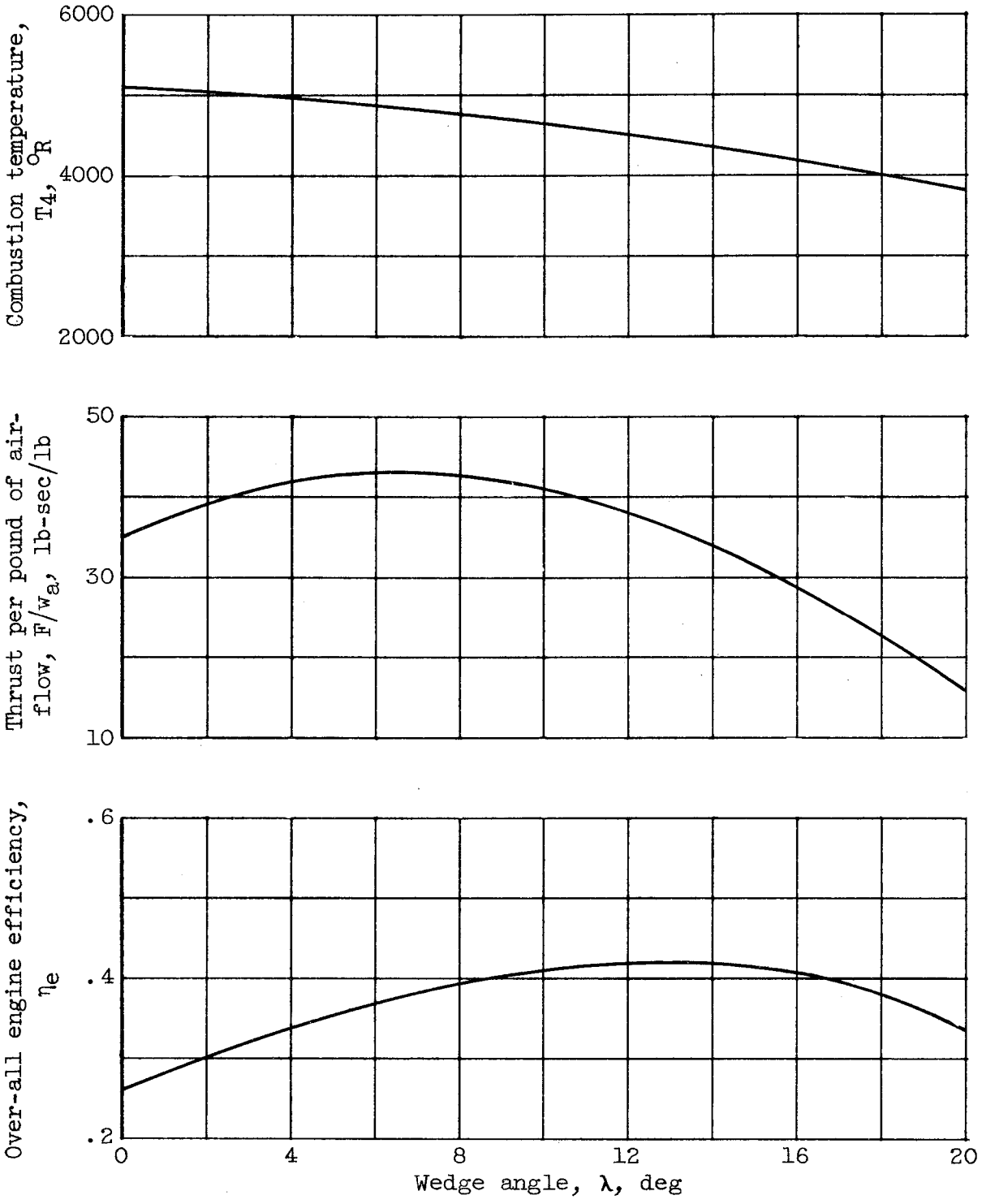

Figure 10. - Effect of inlet wedge angle on performance of SCRJ. M_O, 6.0; A_4/A_2, 1.0; η_c, 0.95; M_4, 1.0; C_V, 0.96; real gas.

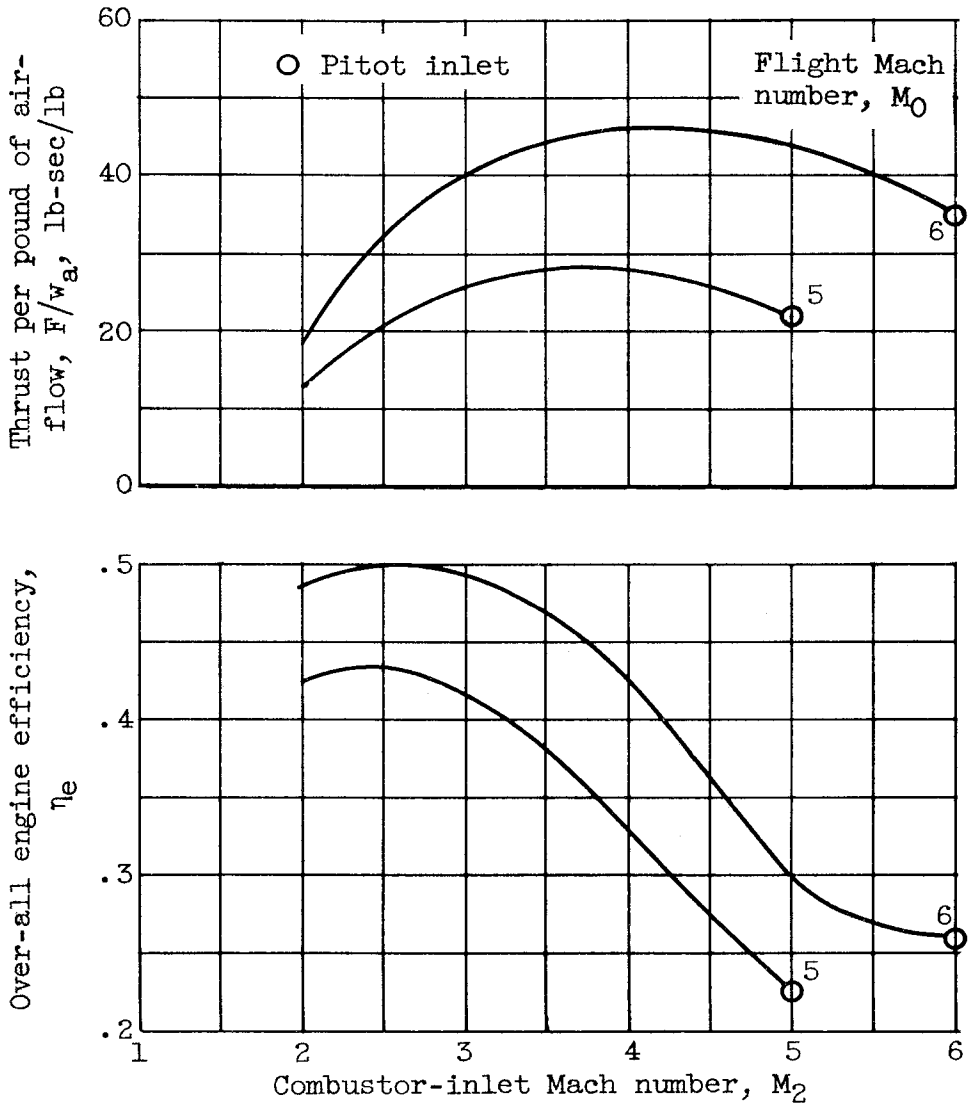

Figure 11. - Effect of combustor-inlet Mach number on performance of SCRJ. Isentropic inlet (P_2/P_0, 1.0); A_4/A_2, 1.0; η_c, 0.95; M_4, 1.0; C_V, 0.96; real gas.

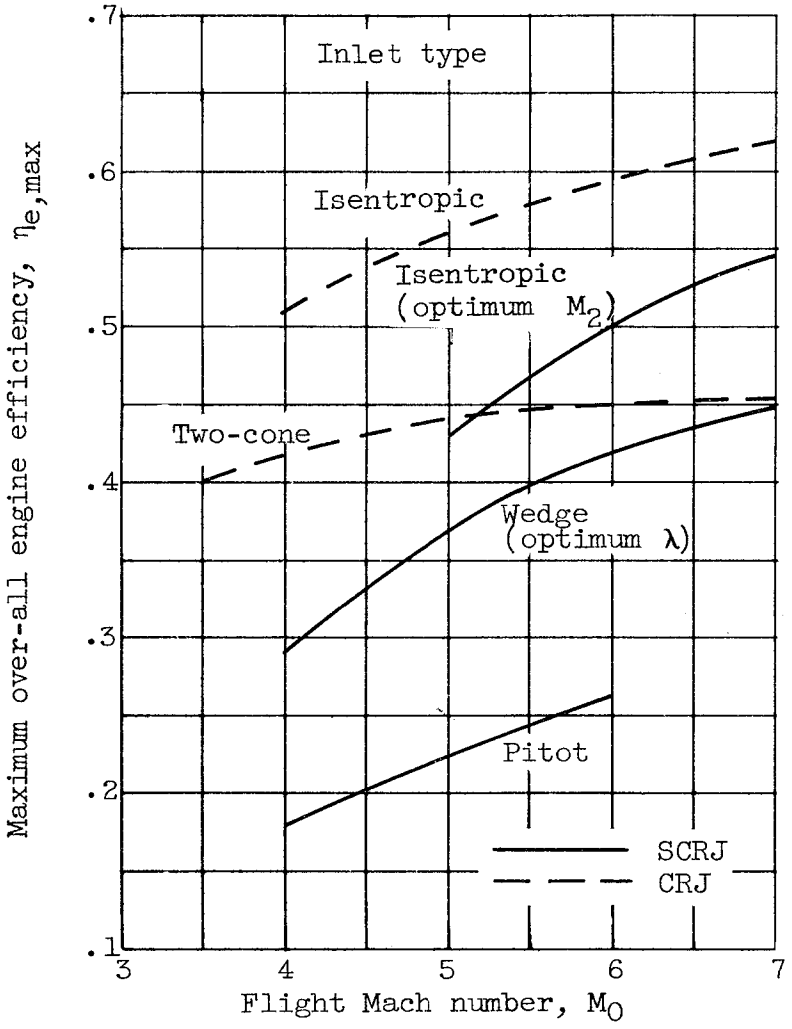

Figure 12. - Comparison of CRJ and SCRJ with various inlet types. A_4/A_2, 1.0; η_c, 0.95; M_4, 1.0 for all SCRJ; C_V, 0.96; real gas.

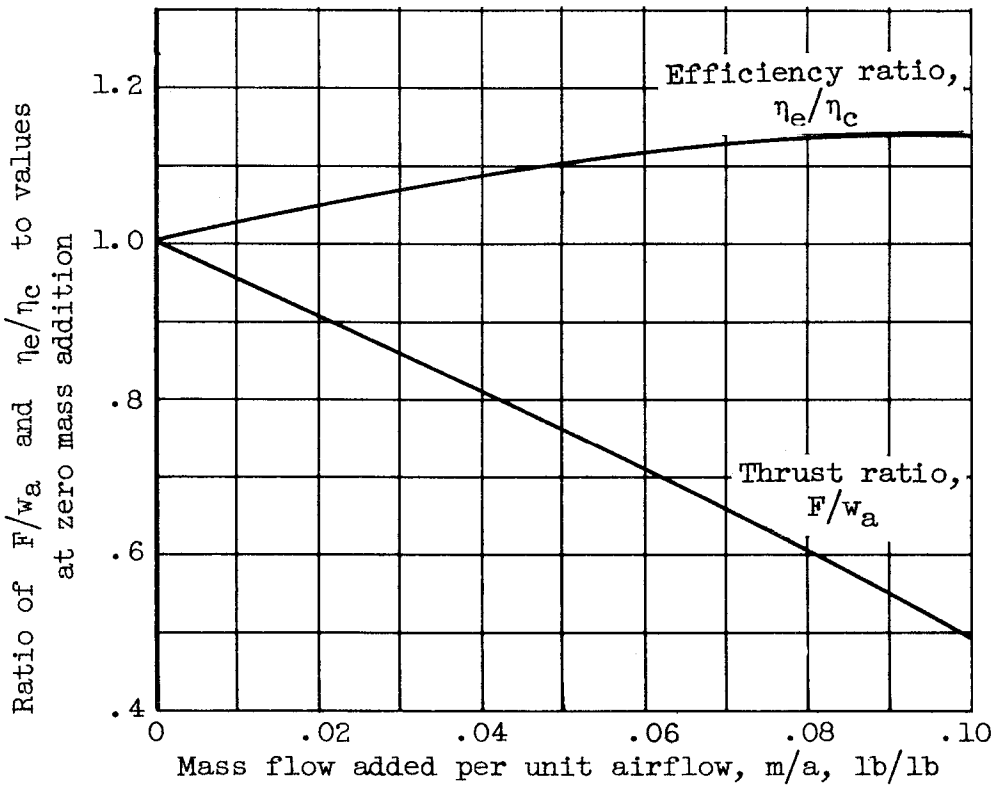

Figure 13. - Effect of mass addition on performance of SCRJ. Pitot inlet; M_0, 6.0; A_4/A_2, 1.0; M_4, 1.0; C_V, 0.96; ideal gas.

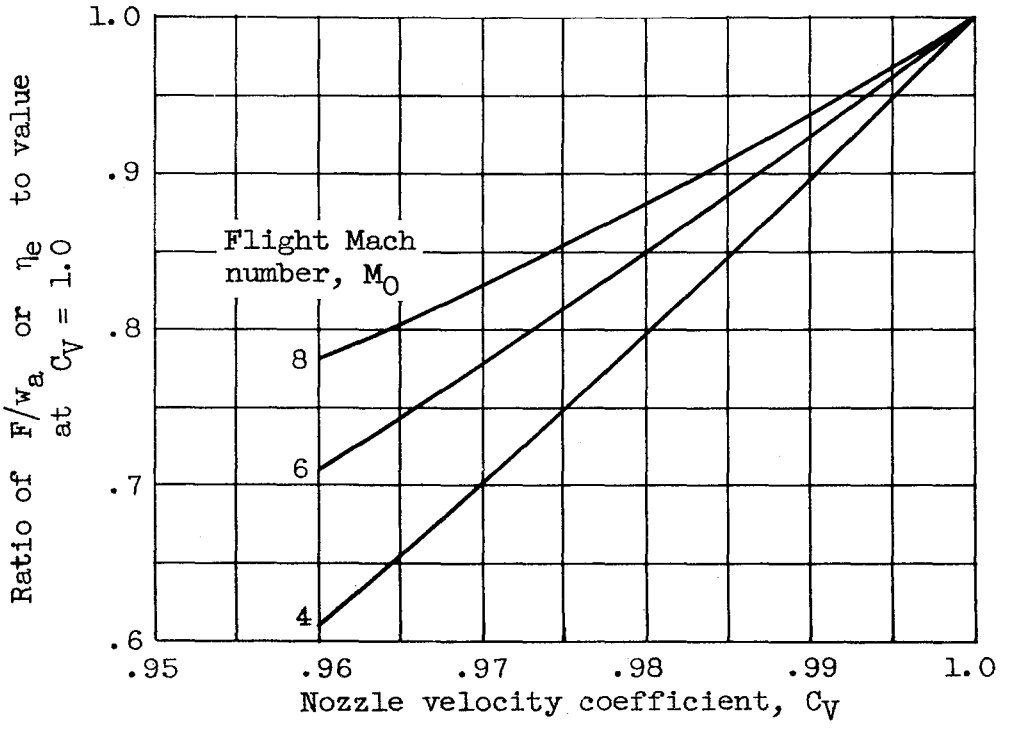

Figure 14. - Effect of nozzle velocity coefficient on performance of SCRJ. Pitot inlet; A_4/A_2, 1.0; M_4, 1.0; ideal gas.

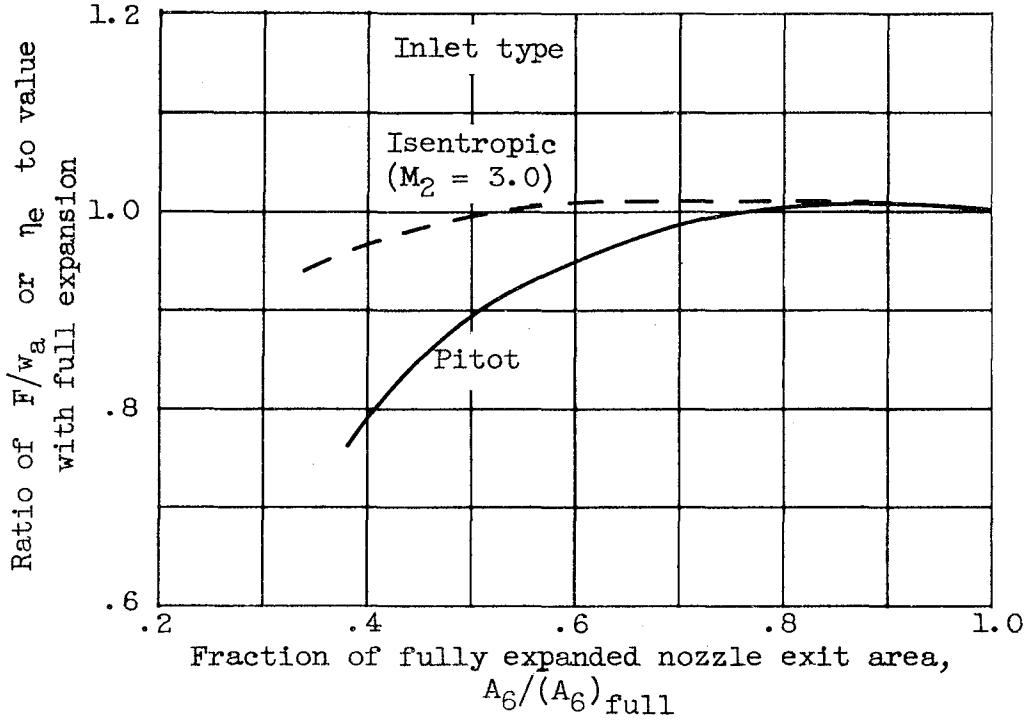

Figure 15. - Effect of incomplete nozzle expansion on performance of SCRJ. M_0, 6.0; A_4/A_2, 1.0; M_4, 1.0; C_V, 0.96; real gas.

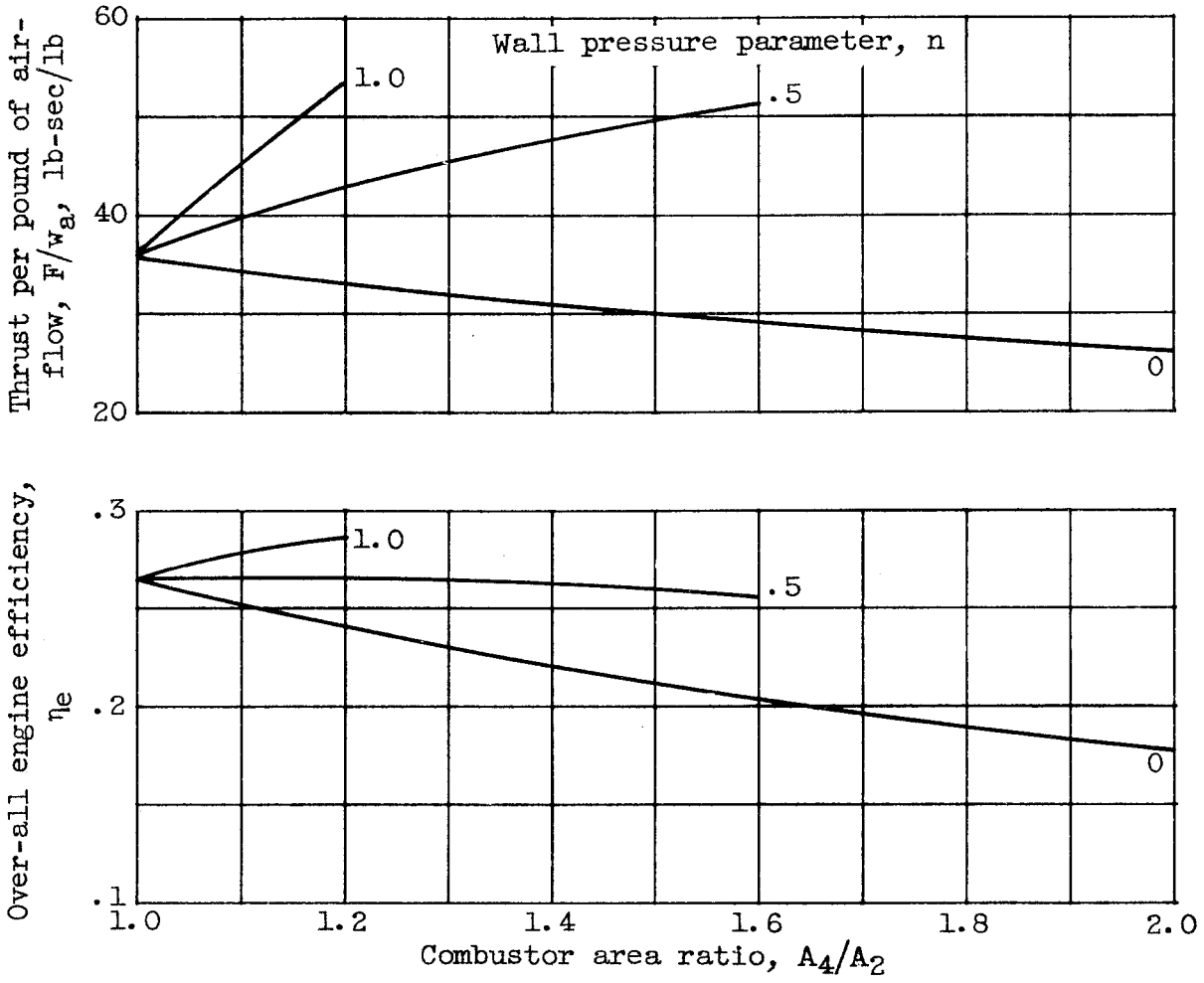

Figure 16. - Effect of combustor area ratio and wall pressure parameter on performance of SCRJ. Pitot inlet; M_O, 6.0; η_c, 0.95; M_4, 1.0; C_V, 0.96; real gas.

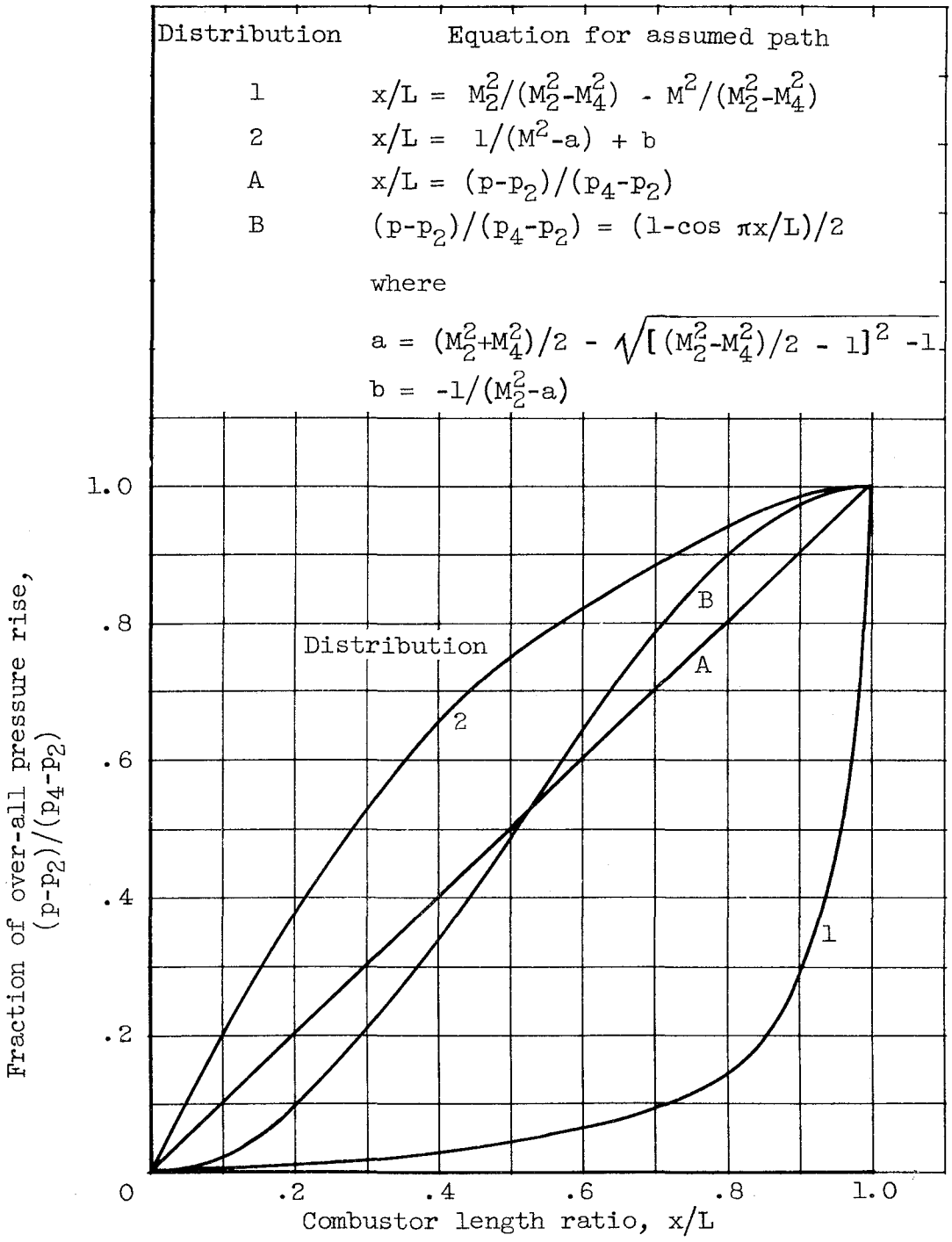

(a) Pressure distribution.

Figure 17. - Various assumed axial property distributions for supersonic combustion in a conical duct. Ideal gas.

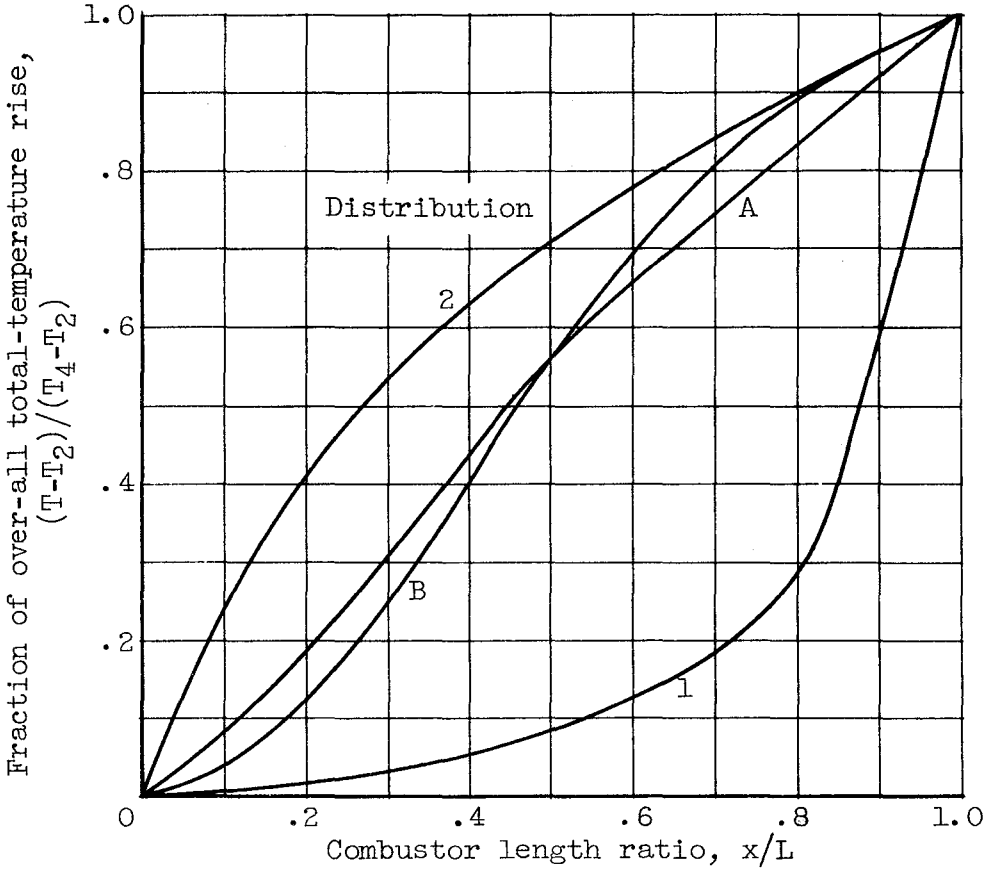

(b) Total-temperature distribution.

Figure 17. - Concluded. Various assumed axial property distributions for supersonic combustion in a conical duct. Ideal gas.

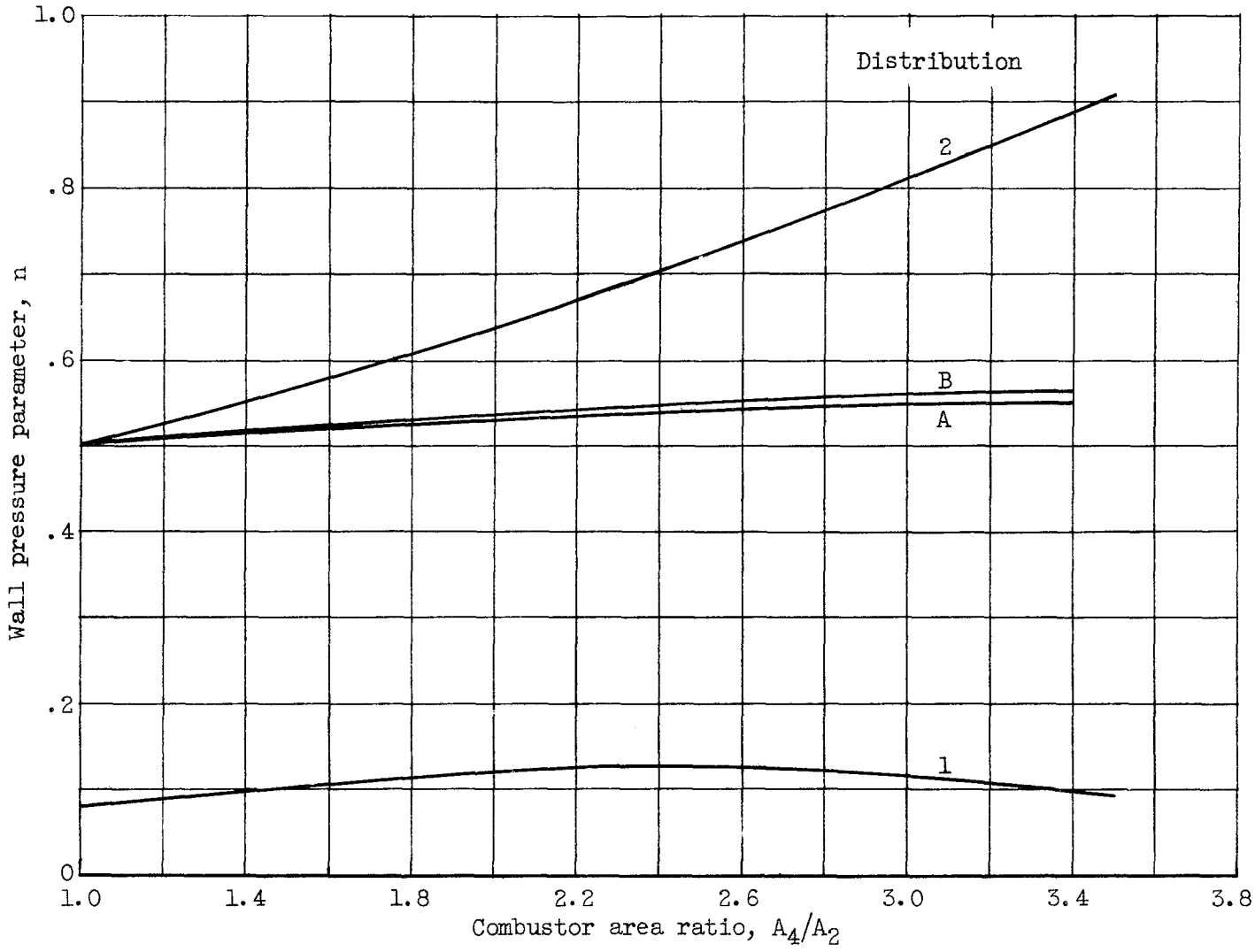

Figure 18. - Values of wall pressure parameter associated with the assumed axial property distributions for supersonic combustion in a conical duct. Ideal gas.

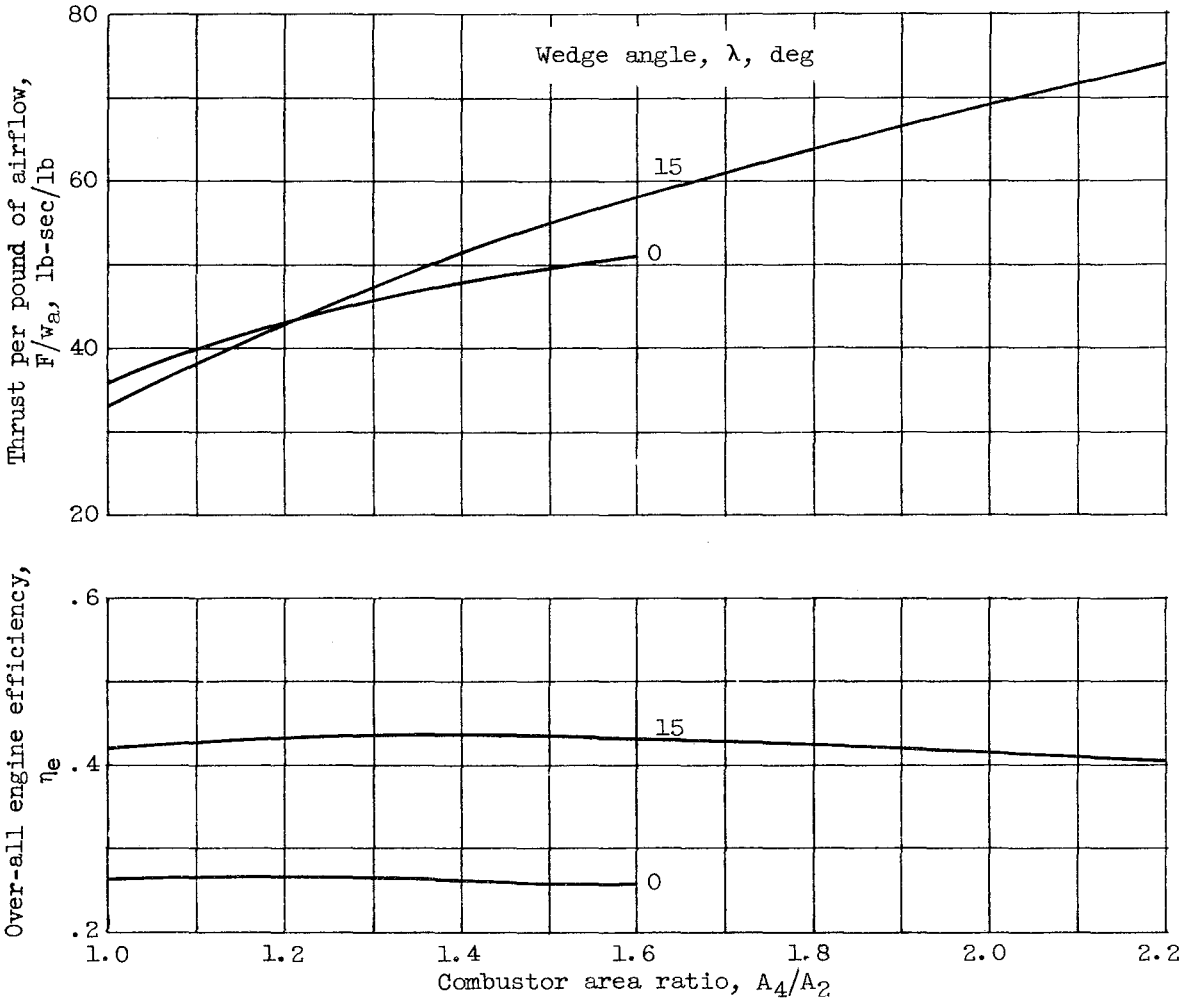

(a) Wedge inlet. Flight Mach number, 6.0.

Figure 19. - Effect of combustor area ratio on performance of SCRJ. η_c, 0.95; n, 0.5; M_4, 1.0; C_V, 0.96; real gas.

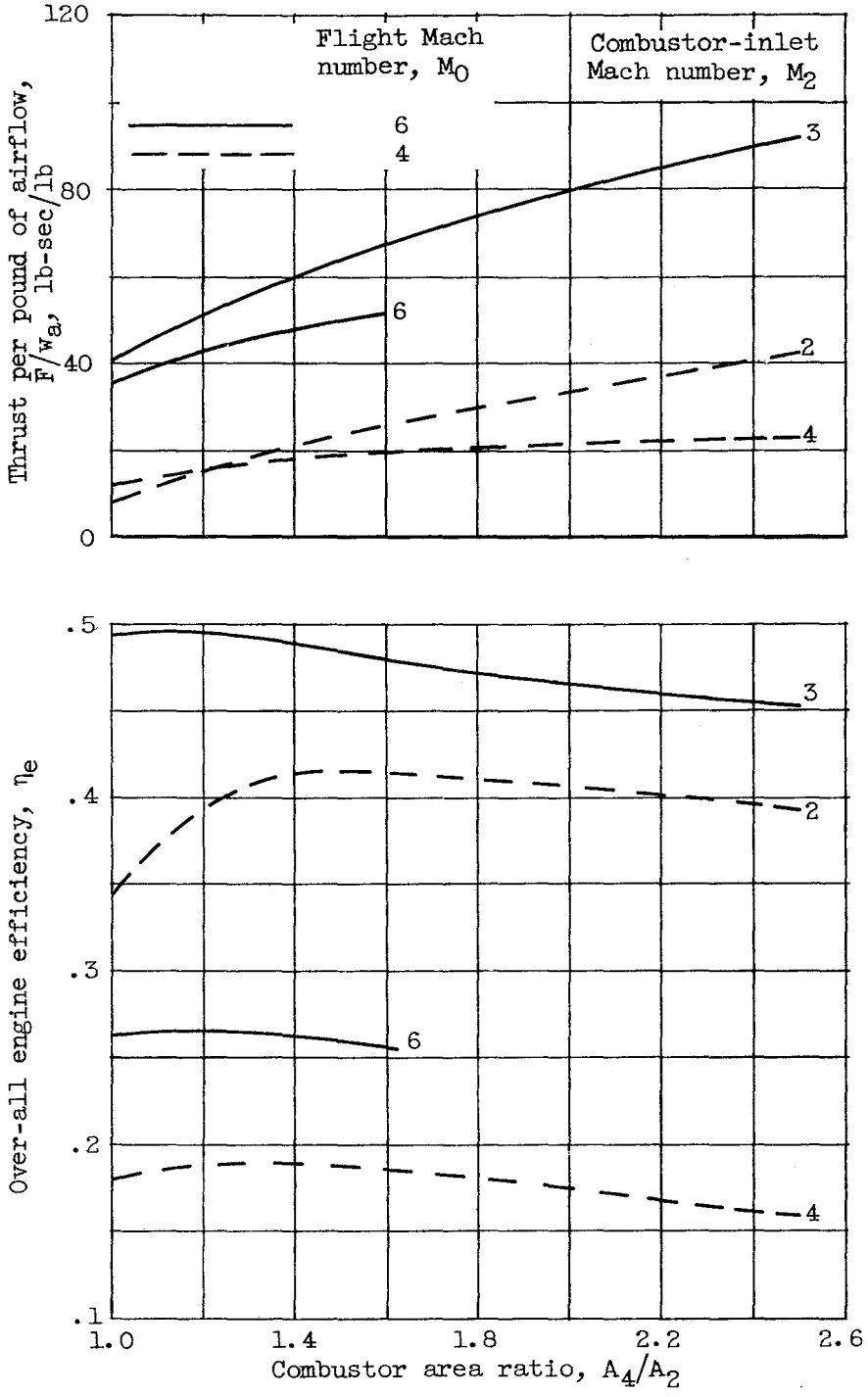

(b) Isentropic inlet.

Figure 19. - Concluded. Effect of combustor area ratio on performance of SCRJ. η_c, 0.95; n, 0.5; M_4, 1.0; C_V, 0.96; real gas.

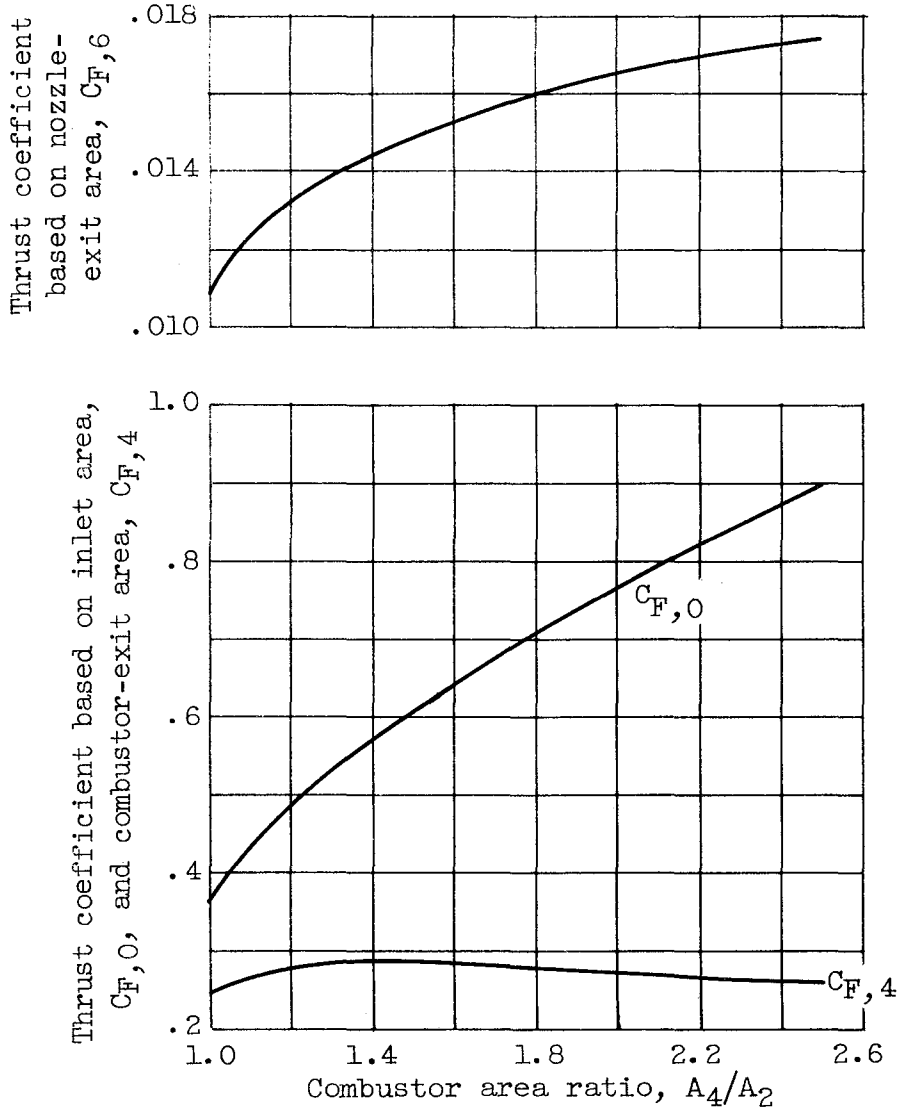

Figure 20. - Effect of combustor area ratio on various SCRJ thrust coefficients. Wedge inlet (λ, 15°); M_0, 6.0; η_c, 0.95; n, 0.5; M_4, 1.0; C_V, 0.96; real gas.

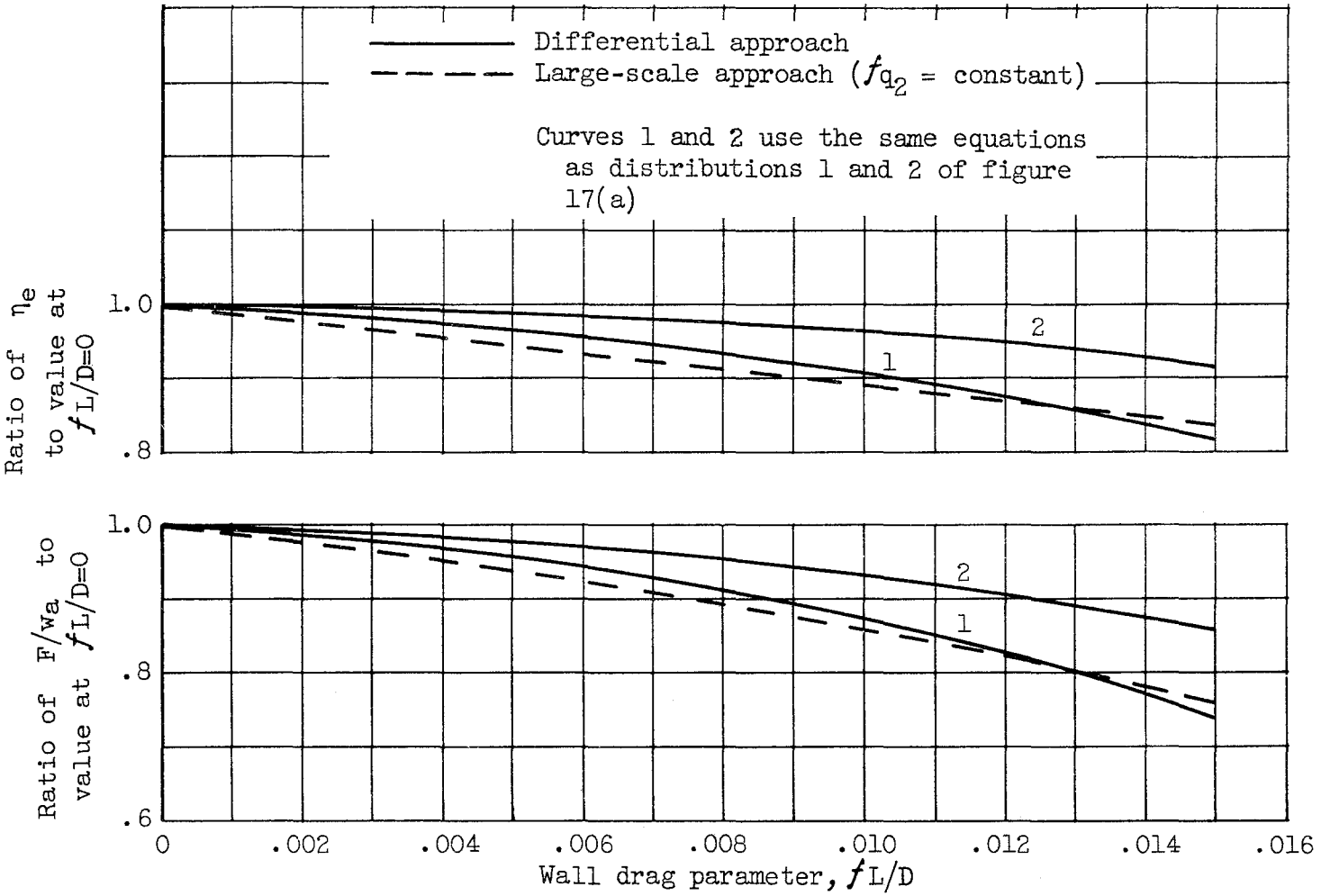

Figure 21. - Effect of assumed path on wall friction losses for SCRJ. Pitot inlet; M_0, 6.0; A_4/A_2, 1.0; M_4, 1.0; C_V, 0.96; ideal gas.

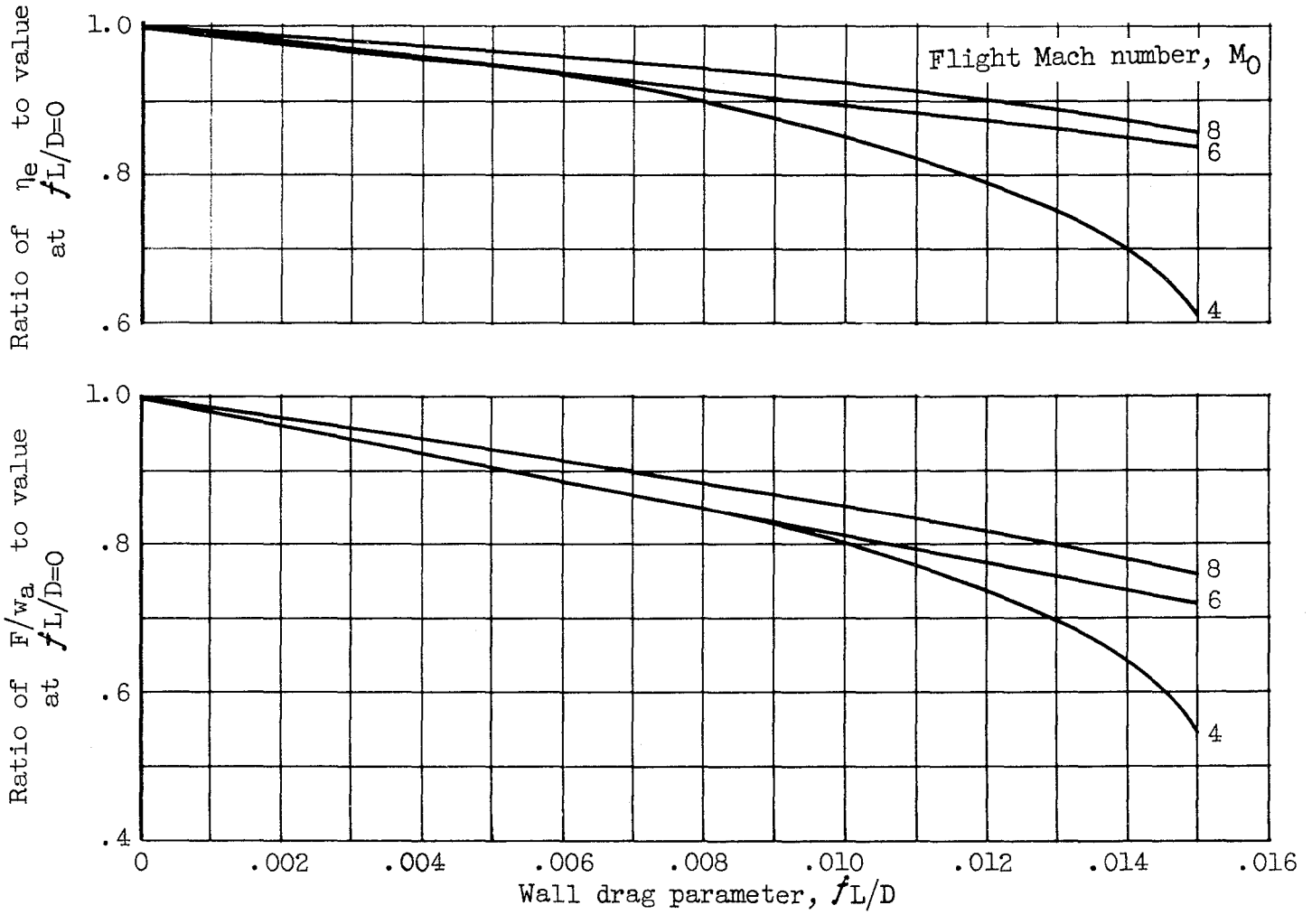

Figure 22. - Effect of wall friction loss on performance of SCRJ. Pitot inlet; A_4/A_2, 1.0; M_4, 1.0; C_V, 0.96; ideal gas.

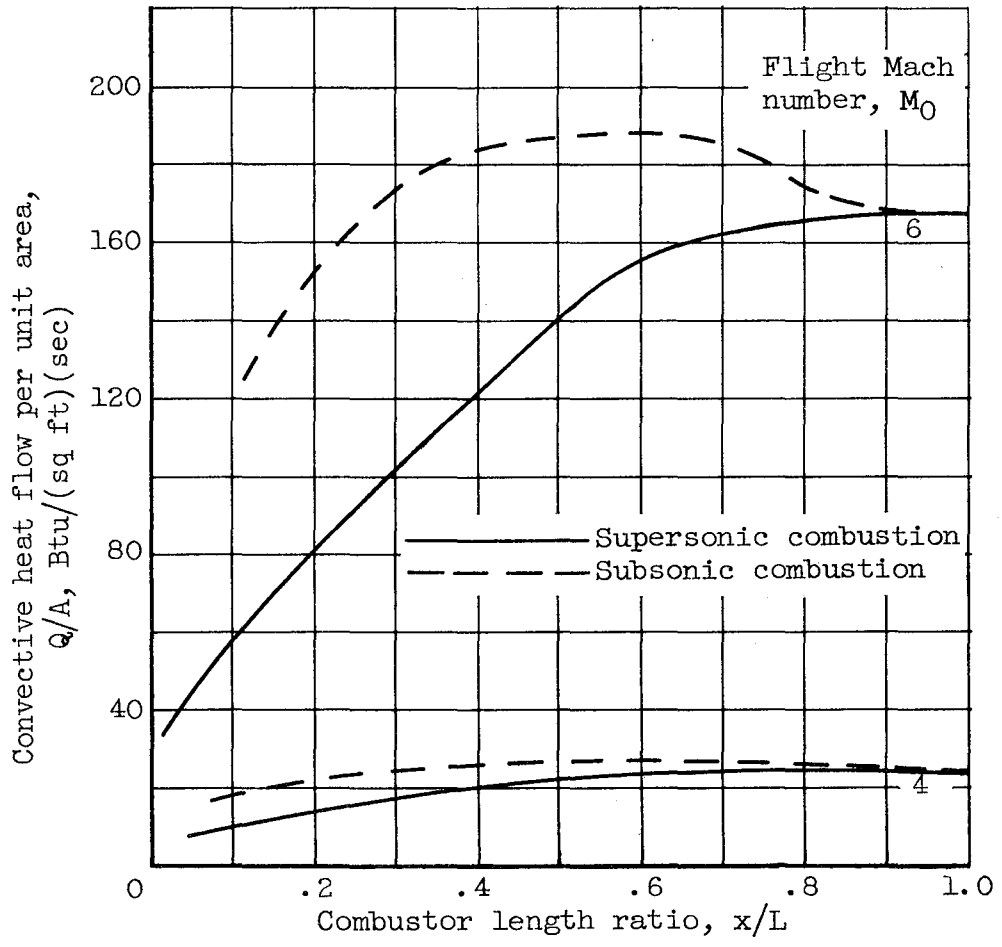

Figure 23. - Comparison of convective heat loads with supersonic and subsonic combustion. Pitot inlet; A_4/A_2, 1.0; L, 5.0 feet; M_4, 1.0; altitude, 60,000 feet.

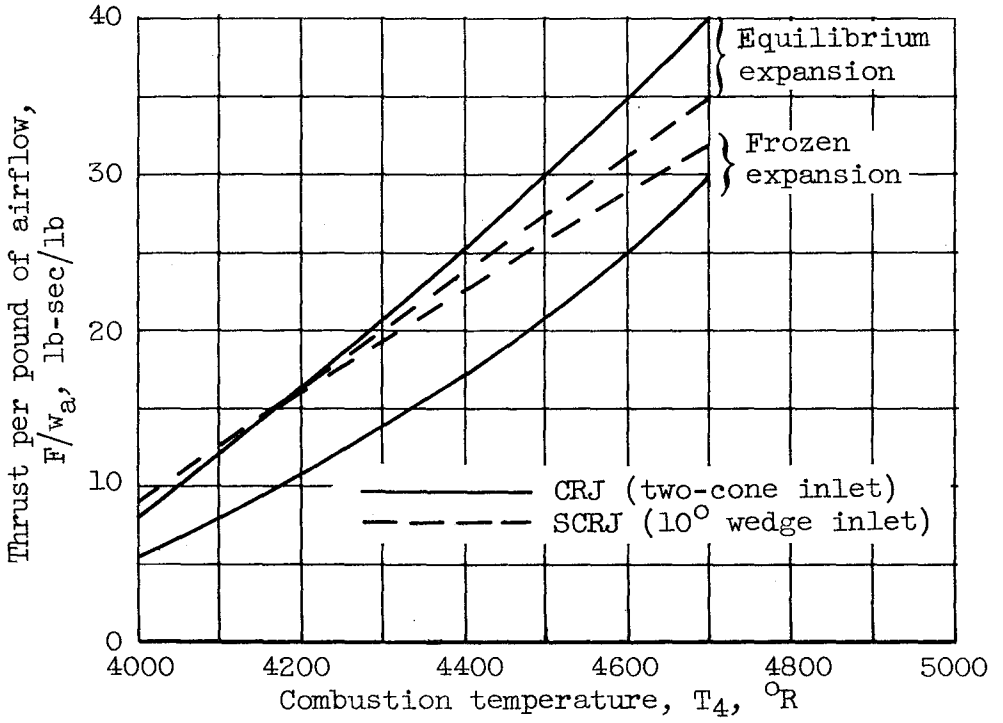

Figure 24. - Performance penalty due to frozen expansion in the exhaust nozzle. Variable specific heat, but no recombination assumed for the frozen case; M_0, 6.0; A_4/A_2, 1.0; altitude, 120,000 feet; C_V, 0.96.